

T.C.
YEDITEPE UNIVERSITY
INSTITUTE OF HEALTH SCIENCES
DEPARTMENT OF MEDICAL PHYSICS

**EVALUATION OF THE LOCALIZATION
ACCURACY OF THE PTV IN SBRT APPLICATIONS
USING VMAT TECHNIQUE FOR MOBILE
TUMOURS THROUGH RETROSPECTIVE
ANALYSIS OF 4D CBCT IMAGES**

JÜLIDE CANBULDU

MASTER THESIS

ISTANBUL-2024

T.C.
YEDITEPE UNIVERSITY
INSTITUTE OF HEALTH SCIENCES
DEPARTMENT OF MEDICAL PHYSICS

**EVALUATION OF THE LOCALIZATION
ACCURACY OF THE PTV IN SBRT APPLICATIONS
USING VMAT TECHNIQUE FOR MOBILE
TUMOURS THROUGH RETROSPECTIVE
ANALYSIS OF 4D CBCT IMAGES**

JULIDE CANBULDU

MASTER THESIS

SUPERVISOR

PROF. DR. ŞERİFE İPEK KARAASLAN
DR. CEMİLE CEYLAN

ISTANBUL-2024

THESIS APPROVAL FORM

Institute: Yeditepe University Institute of Health Sciences

Program: Medical Physics

Title of the Thesis: Evaluation of the Localization Accuracy of the PTV in SBRT Applications Using VMAT Technique for Mobile Tumours Through Retrospective Analysis of 4DCBCT Images.

Owner of the Thesis: Julide Canbuldu

Examination Date: 29.04.2024

This study has been approved as a Master Thesis regarding content and quality by the Jury.

	Title, Name-Surname (Institution)
Chair of the Jury:	Dr. Türkay Toklu, Yeditepe University
Supervisor:	Prof. Dr. Serife Ipek Karaaslan, Yeditepe University
Co-supervisor/Examiner	Dr. Cemile. Ceylan, Istanbul Oncology Hospital, Yeditepe University
Member/Examiner:	Dr. Emel Hacıislamoglu, Karadeniz Teknik University
Member/Examiner:	Dr. Sule Karabulut Gul, Saglik Bilimleri University, Lutfi Kirdar Kartal Hospital

APPROVAL

The jury deemed this thesis in accordance with the relevant articles of Yeditepe University Graduate Education and Examinations Regulation. The institute's Administrative Board approved it with a decision dated numbered

Prof. Dr. Bayram YILMAZ
Director of the Institute of Health Sciences

DECLARATION

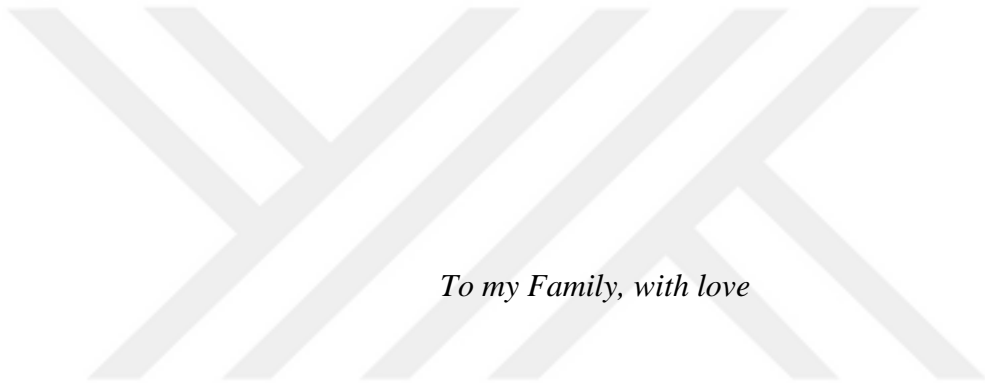
I hereby declare that this thesis is my work and that, to the best of my knowledge and belief, it contains no material previously published or written by another person nor material accepted for the award of any other degree except where due acknowledgment has been made in the text.

29.04.2024

JULIDE CANBULDU



DEDICATION



To my Family, with love

ACKNOWLEDGEMENTS

First and foremost, I would like to thank my esteemed advisor, Prof. Dr. Şerife İpek Karaaslan, who accepted me to this program, allowed me to become a student years later, opened the doors of the academic world, and gave me the chance to write these lines today, believing that everyone can succeed, regardless of age and time, if given the opportunity.

I want to thank my valuable instructors, Dr. Cemile Ceylan and Dr. Türkay Toklu, for their endless patience and effort toward me during my Dissertation process despite their hectic work schedules.

In addition, I am sincerely grateful to my advisor, Dr. Cemile Ceylan, who, despite her troubles, gave me all types of support at the Istanbul Oncology Hospital during my Dissertation experiments. As a medical physicist, her love of research and passion for learning have lit and inspired me on this path.

TABLE OF CONTENTS

THESIS APPROVAL FORM	ii
DECLARATION	iii
DEDICATION.....	iv
ACKNOWLEDGEMENTS.....	v
LIST OF TABLES.....	vii
LIST OF FIGURES.....	ix
LIST OF SYMBOLS AND ABBREVIATIONS.....	xi
ABSTRACT.....	xii
ÖZET	xiii
1. INTRODUCTION AND PURPOSE.....	1
1.1. The History of SBRT.....	2
1.2. Aim of This Thesis	3
2. GENERAL INFORMATION AND LITERATURE REVIEW.....	5
2.1. Stereotactic Body Radiation Therapy (SBRT)	5
2.1.1. Immobilization and Imaging in SBRT	6
2.1.2. SBRT in Treatment Planning.....	8
2.2. Lung SBRT	11
2.2.1. Prescription for Lung SBRT Dose.....	13
2.2.2. Immobilization in Lung SBRT	15
2.2.3. Strategies for Respiratory Motion Management	16
2.2.4. Tumor Motion Definition with Imaging in Lung SBRT	17
2.2.5. Implementing Advanced Techniques in Motion Management for Lung SBRT	24
2.2.5.1. Breath Hold Radiotherapy Techniques.....	26
2.2.5.2. Respiratory Gating Treatment Technique	28
2.3. Image Guided Radiation Therapy (IGRT).....	31
2.3.1. Cone Beam Computed Tomography (CBCT)	32
2.3.2. Four-Dimensional Cone Beam Computed Tomography (4DCBCT)	33
2.4. Volumetric Arc Therapy (VMAT)	37
3. MATERIALS AND METHODS.....	40
3.1. Patient Selection	40

3.2. Simulation and Delineation	41
3.3. Treatment Planning	46
3.4. Treatment	49
3.4.1. Treatment Machine: Elekta Versa HD	49
3.4.2. Treatment Procedure	50
3.4.2.1. 4DCBCT Pre-Treatment and Symmetry Software	50
3.5. Image Transfer and Registration Method	54
3.5.1. 4DCT and 4DCBCT Image Registration	55
3.5.2. Delineation of 4D CBCT to Define GTV Volume.....	56
3.5.3. Comparison of the centroid positions of ITV and GTV_{4DCBCT}	57
4. RESULTS.....	60
4.1.1. Intra-Fraction Motion Evaluation	63
4.1.2. The Motion Amplitude Vector Evaluation Versus Tumor Localization	64
4.1.3. The Motion Amplitude Vector Evaluation Versus Tumor Volume	70
4.1.4. The Evaluation of Motion Amplitude Vector in Relation to Age	74
4.1.5. The Evaluation of Motion Amplitude Vector in Relation to Sex	75
4.2. Summary Statistics and Analysis	76
5. DISCUSSION AND CONCLUSION	77
6. REFERENCES	81
7. CURRICULUM VITAE.....	85

LIST OF TABLES

Table 2.1. Prescription Dosage Conformity in Heterogenous Tissues for Photon	14
Table 2.2. Comparative Overview of Strategies	16
Table 2.3. Comparative Analysis of Techniques	25
Table 3.1. Characteristics of the 19 Patients and Diseases	41
Table 3.2. The Tumor Characteristics and Margins of 19 Patients in This Study	45
Table 3.3. Patient Dose, Fractionation Schedule, and Respective Percentage Coverage Values	48
Table 4.1. The Variation between GTV and ITV Centroid Position	61
Table 4.2. Maximum Centroid Variation, Mean Variation Values in the RL, SI, and AP Coordinates, and The Number of Lesions Greater Than 5 mm.	67
Table 4.3. V_{max} (mm), Tumor Localization and Zone Classification Values of Lesions	68
Table 4.4. Comparison The Variation between ITV (cc) and Mean GTV Volume (cc).....	71
Table 4.5. Comparison V_{max} and Age	74
Table 4.6. Comparison V_{max} and Sex	75

LIST OF FIGURES

Figure 2.1. Vacuum Bag and Thermoplastic Mask	7
Figure 2.2. Schematic ICRU-Defined Volumes and Their Relative Size	9
Figure 2.3. Isodose Lines for Lung Cancer Patients are Delineated for Two Separate Voxels, Isocenter and Peripheral	11
Figure 2.4. Commercially Available Immobilization Devices	15
Figure 2.5. Comparison Between Standard and Slow CT in Peak to Trough Motion of 1.5cm for 4 Images	18
Figure 2.6. An Illustration of How Individual Image Slices Are Transformed into a 4DCT Image Using the Respiratory Signal	19
Figure 2.7. MIP, Min IP, AIP of a Lung Tumor	21
Figure 2.8. An Early-Stage Lung Cancer Patient's 4DCT Images At End-Inhalation (A) And End-Exhalation (B), Along With Combined Outlines From All 10 4DCT Phases (C) Is Displayed	22
Figure 2.9. The Sequences A, B, C, And D Depict Lung Tissue, Metastasis, Diaphragm, And Chest Wall In The Lung Cancer Images.....	23
Figure 2.10. ITV (Yellow) And PTV (Purple) Volumes Obtained By Adding 5mm To The ITV	24
Figure 2.11. Comparison Between (a) ITV Only, (b) Abdominal Compression, (c) Breath Hold or Gating, and (d) Target Tracking	26
Figure 2.12. Spirometer, Active-Breath Holding	27
Figure 2.13. Free Breathing, Breath Hold GTV Margins	27
Figure 2.14. Abdominal Compression	28
Figure 2.15. Retrospective Gating For 4DCT Data Acquisition	30
Figure 2.16. Fiducial Markers in Internal and External Movement	30
Figure 2.17. The Reconstruction Principle of 4DCBCT Involves Using Projections Acquired From 4 Respiratory Phases	34
Figure 2.18. A Control Point in the Planning System, with a Fluence Map in Greyscale and Precisely Segmented MLC Leaves	38
Figure 2.19. Axial, Sagittal, And Coronal Images For A 180-VMAT Plan. The Pink Shaded Structure Represents ITV, And The Green Shaded Are Represents PTV.....	39
Figure 3.1. Immobilization of Patient Using (A) a Wing Board, (B) a Vacuum Bag and Abdominal Compression	42

Figure 3.2. Utilizing a Wire to Create the Respiratory Pattern During the 4DCT.....	43
Figure 3.3. Treatment Plan and the Corresponding DVH Values	46
Figure 3.4. Treatment Plan of Two Different Lesions and Their Corresponding DVH Values	47
Figure 3.5. DVH Statistics	47
Figure 3.6. Istanbul Oncology Hospital; LINAC Device, Elekta Versa HD	50
Figure 3.7. 4DCBCT Symmetry Protocol Clip Box Matching: Bony Structure	52
Figure 3.8. Mask Matching: Mapping ITV for Each Phase of Respiration	52
Figure 3.9. Correlation Of Position Errors Obtained From Clipbox And Mask Registration	53
Figure 3.10. Transmission Of 4DCBCT Images To The Monaco Treatment Planning System Using Back Projection	54
Figure 3.11. Matching 4DCT And 4DCBCT Images For A Single Fraction With A Diaphragm Lesion In A Patient	55
Figure 3.12. Delineation Of GTV For A Single Fraction Of 4DCBCT And ITV In 4DCT Images, With Using Lung Window Level In A Diaphragm Lesion	57
Figure 3.13. Place Interest Points For Calculating The Centroid Positions In The 4DCBCT And ITV Fusion Images For A Diaphragm Lesion	58
Figure 3.14. The Variation Between Centroid Positions Of ITV And GTV_{4DCBCT} In (x-y) Coordinates	60
Figure 4.1. The Standard Deviation In The RL Position	65
Figure 4.2. The Standard Deviation In The SI Position	66
Figure 4.3. The Standard Deviation In The AP Position	66
Figure 4.4. The Standard Deviation Of V_{Max}	67
Figure 4.5. Comparison of Maximum Variations by Tumor Localization	69
Figure 4.6. Maximum Variations in Lesion Localization of Patients	70
Figure 4.7. ITV Volume Vs Mean GTVx Volume with Trend Line	72
Figure 4.8. Mean GTV Volumes Across Different Lesions	73
Figure 4.9. Age and V_{max} Variation	74

LIST OF SYMBOLS AND ABBREVIATIONS

AIP	:	Average Intensity Projection
AP	:	Anterior Posterior
CBCT	:	Cone Beam Computed Tomography
CTV	:	Clinical Target Volume
DVH	:	Dose-Volume Histogram
FFF	:	Flattening-filter free
FOV	:	Field of View
GTV	:	Gross Tumor Volume
Gy	:	Gray (Radiation Unit)
IGRT	:	Image Guided Radiation Therapy
IMRT	:	Intensity-Modulated Radiotherapy
ITV	:	Internal Target Volume
LINAC	:	Linear Accelerator
MIP	:	Maximum Intensity Projection
Min-IP	:	Minimum Intensity Projection
MLC	:	Multi-leaf Collimator
OAR	:	Organ at Risk
PTV	:	Planning Target Volume
RL	:	Right Left (Direction)
RTOG	:	Radiation Therapy Oncology Group
SBRT	:	Stereotactic Body Radiation Therapy
SI	:	Superior Inferior (Direction)
TPS	:	Treatment Planning System
VMAT	:	Volumetric Arc Therapy
4DCBCT	:	Four-Dimensional Cone Beam Computed Tomography
4DCT	:	Four-Dimensional Computed Tomography

ABSTRACT

Canbuldu, J. (2023). Evaluation of the Localization Accuracy of the PTV in SBRT Applications Using VMAT Technique for Mobile Tumours Through Retrospective Analysis of 4DCBCT Images. Yeditepe University, Institute of Health Science, Department of Medical Physics, MSc thesis, Istanbul.

Stereotactic body radiotherapy (SBRT) is a highly precise radiation therapy technique used to treat mobile tumors, especially lung cancers. This thesis examines the accuracy of locating the planned target volume (PTV) in SBRT applications using volumetric modulated arc therapy (VMAT) for mobile tumors. The study involves analyzing 4-dimensional cone beam computed tomography (4DCBCT) images. SBRT has become popular over the past two decades due to its ability to precisely deliver high doses of radiation to the tumor while minimizing exposure to surrounding healthy tissue. This precision is achieved through hypofractionated treatment and advanced imaging technologies that enable accurate tumor localization. The effectiveness of SBRT in treating lung cancers heavily relies on the precise alignment and delivery of radiation beams, which is challenging due to tumor motion caused by respiration and other factors. Various methods have been developed to reduce patient positioning and tumor motion uncertainties, including the breath-hold technique, forced shallow breathing method, respiratory gating, and real-time tracking. 4DCBCT has become a crucial tool, offering improved accuracy in tumor localization by tracking the tumor's path over multiple respiratory phases. This technology creates highly accurate gross target volumes (GTVs) that can be verified before each treatment fraction, ensuring precise alignment and dosage delivery. The aim of this thesis is to evaluate the accuracy of localizing mobile tumors using 4DCBCT imaging during SBRT. The retrospective study involves a detailed assessment of setup errors and tumor motion during beam delivery for patients undergoing VMAT-SBRT. By analyzing 4DCBCT images, the study seeks to determine the adequacy of the PTV margins and the effectiveness of this imaging modality in improving the treatment planning process. This research provides a comprehensive understanding of the potential of 4DCBCT imaging to enhance the precision of tumor localization and optimize treatment outcomes for patients with mobile tumors.

Keywords: SBRT, VMAT, CBCT, 4DCBCT, PTV

ÖZET

Canbuldu, J. (2023). Hareketli tümörlerin volumetrik ark radyoterapi tekniği (VMAT) ile planlanan stereotaktik vücut radyoterapi (SBRT) uygulamalarında, planlanan hedef hacmin (PTV) lokalizasyon doğruluğunun 4 boyutlu cone beam bilgisayarlı tomografi (4DCBCT) görüntüleri kullanılarak değerlendirilmesi. Yeditepe Üniversitesi Sağlık Bilimleri Enstitüsü, Medikal Fizik ABD, Master tezi, İstanbul.

Stereotaktik vücut radyoterapisi (SBRT), özellikle akciğer kanserleri olmak üzere, hareketli tümörlerin tedavisinde kullanılan hassas bir radyoterapi tekniğidir. Bu tez, hareketli tümörler için hacimsel modüle ark terapisi (VMAT) kullanarak SBRT uygulamalarında planlanan hedef hacmin (PTV) yerleştirilme doğruluğunu incelemektedir. Çalışma, 4 boyutlu konik ışınlı bilgisayarlı tomografi (4DCBCT) görüntülerinin analizini içermektedir. SBRT, yüksek radyasyon dozlarını tümöre hassas bir şekilde iletme ve çevresindeki sağlıklı dokuyu minimum düzeyde etkileme kabiliyeti nedeniyle son yirmi yılda popülerlik kazanmıştır. SBRT'nin akciğer kanserlerini tedavi etmedeki etkinliği, tümör hareketi nedeniyle ortaya çıkan zorluklar nedeniyle, radyasyon ışınlarının doğru hizalanmasına ve iletimine dayanır. Hasta pozisyonlama ve tümör hareketi ile ilgili belirsizlikleri azaltmak için çeşitli yöntemler geliştirilmiştir. 4DCBCT, tümörün yolunu birden fazla solunum fazında izleyerek tümör lokalizasyonunda iyileştirilmiş doğruluk sunan önemli bir araç haline gelmiştir. Bu teknoloji, her tedavi fraksiyonu öncesinde doğrulanabilecek son derece doğru iç hedef hacimleri (GTV'ler) oluşturmayı sağlar ve böylece hassas hizalama ve doz iletimini güvence altına alır. Bu tezin amacı, SBRT sırasında 4DCBCT görüntüleme kullanarak hareketli tümörlerin lokalizasyon doğruluğunu değerlendirmektir. Retrospektif çalışma, VMAT-SBRT uygulanan hastalarda kurulum hatalarını ve ışın iletimi sırasında tümör hareketini detaylı bir şekilde değerlendirmeyi içermektedir. 4DCBCT görüntülerini analiz ederek, PTV marjlarının yeterliliğini ve bu görüntüleme modülünün tedavi planlama sürecini iyileştirmedeki etkinliğini belirlemeyi amaçlamaktadır. Bu araştırma, 4DCBCT görüntülemenin tümör lokalizasyon hassasiyetini artırma ve hareketli tümörlere sahip hastalar için tedavi sonuçlarını optimize etme potansiyelini kapsamlı bir şekilde anlamayı sağlamaktadır

Anahtar Kelimeler: SBRT, VMAT, 4DCBCT, PTV

1.

INTRODUCTION AND PURPOSE

Even though radiation has existed in our world for a long time, its exploration, efficiency, and correct usage in medicine have taken lots of years. Radiation in cancer treatment has led to significant progress in medicine by killing cancer cells or halting their growth. Present-day radiotherapy is a treatment method that is widely used to treating cancer efficiently, and reliably. This treatment method ensures the prolongation of survival and increases the quality of life. Some forms of radiation used in treatments are high-energy X-rays, neutrons, protons, electron beams, radioactive sources (α , β , γ emitters), pi-mesons, and heavier charged ions (such as ^{12}C , ^{20}Ne).

Radiotherapy's main goal is delivering the highest possible dose to the specific target region while maximizing tumor control. During that time, it is aimed at the minimum possible damage to organs at risk and surrounding tissues⁽¹⁾.

Radiotherapy is used in cancer treatment to stop tumor cell division and to destroy tumor cells via radiation. This method is the only treatment for some cancer patients. It is also used in addition to treatment to reduce the risk of recurrence of the tumor area after surgical procedures and to increase the effectiveness of treatment in patients who receive low-dose chemotherapy. By combining radiotherapy with other treatment modalities, the overall efficacy of cancer treatment can be significantly improved, offering patients a better chance of recovery and long-term survival.

The advancements in radiotherapy techniques, such as the development of more precise delivery methods and the ability to target tumors with higher accuracy, have greatly contributed to the success of this treatment. Modern technologies, including advanced imaging techniques and computer-assisted planning systems, have revolutionized the way radiotherapy is administered, allowing for more precise targeting of tumors and sparing of healthy tissues. These innovations have not only increased the effectiveness of radiotherapy but have also reduced the side effects associated with treatment, thereby improving the quality of life for patients undergoing therapy.

In conclusion, radiotherapy has become a cornerstone in the treatment of cancer, offering an effective and reliable method to control and eradicate tumors. Its ability to deliver targeted doses of radiation with precision has led to significant improvements in patient outcomes. As research and technology continue to advance, the potential for radiotherapy to

further enhance cancer treatment remains promising, providing hope for even better results in the future.

1.1. The History of SBRT

In 1895, Wilhelm Conrad Rontgen discovered X-rays while researching cathode rays. A few months later, Antoine Henri Becquerel discovered natural radioactivity. In 1898, Pierre-Marie Curie couple found the element radium, which is the natural source of high energy photon or γ rays ⁽²⁾. These three major discoveries can be considered as the fundamentals and milestones of the clinical radiotherapy.

Thanks to neurosurgeon Lars Leksell, the concept of stereotactic met with radiotherapy in 1951 ⁽³⁾. He treated patients by using stereotactic frame and X-rays together and concluded that the stereotactic method increases the quality of treatment even in difficult situations for example brain, since it is hard to get deep inside. Thus, stereotactic radiosurgery (SRS) and stereotactic radiotherapy (SRT) were formed. In 1968 Leksell and his friends invented the gamma-knife device and started to treat their patients with it ⁽³⁾. When performed to treat body tumors, SRT was renamed as stereotactic body radiotherapy (SBRT).

Since X-rays are two dimensional, they were incapable of measuring the depth of the object and drawing the soft tissue of the body. The necessity of increasing the quality of the images taken with X-rays had inspired the invention of Computer Tomography (CT) device in the early 1970s⁽⁴⁾. Thus, in patient monitoring, instead of two-dimensional conventional radiotherapy, CTs that allows three-dimensional monitoring were used.

In the 1980s, Multi-Leaf Collimators (MLCs) were invented ⁽²⁾. MLCs consist of many small leaves, each of which can be individually controlled. These leaves can be positioned precisely based on the size and shape of the treated area to prevent radiation from spreading to unintended areas. This made MLCs a standard procedure for 3D conformal radiotherapy (3DCRT). The development of conformal radiotherapy techniques provided more complex three-dimensional treatment plans. Conformal radiotherapy allows for high radiation exposure to the tumor cells while keeping the radiation exposure to the surrounding normal tissues at a minimum level. Despite advancements in conformal radiotherapy, studies have shown lower rates of local control and overall survival, particularly in early stage non-small cell lung cancer (NSCLC) ⁽⁵⁾ and the high doses delivered with conformal techniques have created significant toxicity ⁽⁶⁾. This indicates that further developments are necessary

for ensuring the best possible outcomes for patients, despite the fact that conformal radiotherapy is a substantial improvement over conventional radiotherapy.

In the 1980s, Intensity-Modulated Radiation Therapy (IMRT) was also developed. This advanced therapy allowed for a more customized approach to radiation treatment by enabling the intensity and shape of the radiation field to be adjusted. As a result, the therapy was better suited to the complexity of the treated tumor and helped to preserve surrounding tissues. However, IMRT treatment takes longer time to complete and can be uncomfortable for patients. Also, any changes in tumor position during both inter- and intra-fraction, or alterations in tumor size or shape over time, can negatively impact the treatment process. Studies have shown that the use of IMRT for lung cancer treatment results in slower reception, and that the small margins provided for the PTV are insufficient for treatment ⁽⁵⁾. Additionally, patients exposed to higher monitor units (MU) during IMRT treatment may be at an increased risk of developing secondary cancer due to radiation exposure ⁽⁷⁾.

In radiotherapy, there is a growing focus on considering respiratory and organ movements to minimize radiation exposure to healthy tissue while delivering a sufficient dose to the intended target. Technological advancements such as linear accelerators and computer-based planning software have contributed to making radiotherapy more precise and effective. These advancements have led to the emergence of SBRT, which is one of the most advanced conformal radiotherapy techniques available today. SBRT is a promising advancement in radiation therapy and shows great potential in improving patient outcomes

1.2.Aim of This Thesis

Our study was focused on determining the planning target volume (PTV) margins for a cohort of 19 lung cancer patients who underwent stereotactic body radiation therapy (SBRT). To achieve this, we incorporated a variation margin to the gross tumor volume to internal target volume (GTV-ITV) obtained using 4D-computed tomography (CT). Subsequently, we utilized 4D-cone beam CT (CBCT) images acquired prior to treatment to evaluate the precision of the irradiated PTV margins.

Lesions were carefully examined in four distinct regions: peripheral, central, diaphragm-adherent, and chest wall-adherent. We employed 4DCBCT to thoroughly assess the adequacy of PTV margins for all planned tumor volumes, encompassing tumors located in various regions.

To ensure precision, the acquired 4D CBCT images were seamlessly transferred to the planning system through back projection. Subsequently, each 4DCBCT image obtained from every fraction of the patient's SBRT was meticulously registered to the planning system with the 4DCT images obtained during the planning phase, allowing for a comprehensive evaluation of our motion management techniques.

Overall, the primary objective of our study was to enhance the accuracy of PTV margin determination for lung cancer patients undergoing SBRT. Through the incorporation of clinical margins to the GTV-ITV, along with the utilization of advanced 4D imaging techniques, we were able to meticulously evaluate the accuracy of PTV margins and refine our motion management approach.

2. GENERAL INFORMATION AND LITERATURE REVIEW

2.1. Stereotactic Body Radiation Therapy (SBRT)

Stereotactic Body Radiation Therapy (SBRT), a breakthrough in precision cancer treatment, originated in the early 1990s at Sweden's Karolinska Institute. SBRT is an advanced form of external beam radiotherapy that delivers high doses of radiation accurately to the targeted body area with millimeter precision. This method is typically non-invasive, provides a high biologically effective dose (BED), and involves 1 to 5 hypo-fractionated treatments⁽⁸⁾. This treatment modality is particularly effective for various lung, liver, spine, neck, lymph nodes, and soft tissue tumors. With hypo-fractionated treatment, the repopulation rate in tumor cells can be reduced. Also, the time the patient spends on the device is decreased, thus improving the patient's comfort and reducing the cost⁽⁹⁾.

Uncertainties regarding respiratory and organ movements are major problems during radiotherapy treatment planning and delivery. Respiratory motion significantly impacts the precision of radiation therapy, introducing complexities in accurately localizing lung tumors and critical structures. The following points elucidate the critical aspects of respiratory motion:

Diaphragm Motion: Primary driver of respiratory movement, affecting the position of lung tumors and nearby organs.

Tumour Localization and Site: Tumours located in the lower lung exhibit the largest motion, up to 50 mm, due to their proximity to the diaphragm. The size of the Gross Tumor Volume (GTV) and the T stage of the disease also play crucial roles⁽¹⁰⁾.

Upper Abdominal Organ Movement: Due to respiratory motion, organs such as the liver, kidneys, and spleen experience significant displacement, typically more than 10 mm⁽¹⁰⁾.

Respiratory motion is influenced by various factors, and it is important to have a comprehensive understanding of it for effective motion management. SBRT is a complex radiotherapy method that uses motion management and image guidance to treat relatively small and mobile tumors in spinal and paraspinal sites located at thoracic and abdominopelvic cavities. Nowadays, SBRT is a widely-used treatment option for various types of cancer, including early-stage non-small cell lung cancer, as well as tumors in the lung, liver, prostate,

and pancreas⁽¹¹⁾. It is also an effective method for treating tumors that have metastasized to the liver, bone, and brain⁽¹¹⁾.

One of the differences between stereotactic body radiation therapy and conventional radiotherapy is the formation of a high biologically effective dose (BED) on a tumor when induced with high radiation for every few fractions. The toxicity caused by a high radiation dose can harm surrounding normal tissues. While the high doses, ranging from 5 to 30 Gy per fraction, are effectively delivered to the target, organs at risk (OARs) containing the lungs, airways, heart, spinal cord, great vessels, esophagus, brachial plexus should be protected by providing a rapid dose fall off⁽¹²⁾. Studies showed that reaching a high BED improves overall survival and local tumor control rates for many tumors. SBRT is generally well-tolerated with minimal risk of severe toxicity, thanks to stringent dose constraints that protect surrounding healthy tissues. For central tumors, 4-5 fraction regimens are recommended to reduce toxicity, while ultra-central tumors are advised against SBRT⁽¹¹⁾.

SBRT is a cancer treatment that is generally well-tolerated by patients. However, a small percentage of patients may experience grade 3 radiation pneumonitis⁽¹³⁾. Therefore, it is crucial to select patients and plan their treatment carefully. SBRT uses advanced immobilization and imaging technology, such as CT scans, to create personalized treatment plans that target cancerous cells while minimizing damage to healthy tissue. With the advent of the MRI-linac, tumors can be visualized in real-time, which enhances the accuracy of radiation delivery. SBRT is a highly sophisticated approach that provides a significant advancement for patients battling cancer by offering a vital option in fewer sessions.

2.1.1. Immobilization and Imaging in SBRT

Changes in target position due to motility, failure to account for set-up errors, and the therapy machine's mechanical and dosimetric limitations cause the dose given to the patient to be different than planned⁽¹²⁾.

The primary purpose of immobilization is to ensure consistent patient positioning throughout the treatment and to minimize uncertainties in patient positioning⁽⁹⁾. Attention should be paid to consistent patient positioning between fractions and minimizing intra-fractional motion as much as possible. Techniques like SBRT require more secure immobilization compared to conventional treatments. In the case of SBRT, patient positioning is critical. Even small positioning errors can lead to permanent, systemic errors due to the high radiation dose delivered in a few fractions⁽¹⁴⁾. Additionally, the risk of

movement during treatment increases due to the longer duration of the treatment compared to traditional radiation therapy. When selecting an immobilization device, it is crucial to prioritize patient comfort, ensure ease of setup, and choose one that permits reduced margins around the tumor.

There are a variety of immobilization devices available for different purposes. For instance, thermoplastic masks are custom-made to fit the patient's head and neck, providing precise immobilization. Shoulder immobilization boards are another popular option that makes securing the patient's movements easy. For breast cancer treatment, there are different types of breast boards tailored to inclined planes or supine positions. Wing boards are used for lung immobilization, while knee cushions help to stabilize the patient's lower extremities. Additionally, vacuum bags are used for whole-body or regional immobilization, ensuring the patient remains fixed during radiation therapy.



Figure 2.1. Vacuum Bag and Thermoplastic Mask

Imaging techniques play a crucial role in ensuring the precision and accuracy of treatment in all modern radiotherapy. This is especially true in SBRT, where high-quality imaging with exceptional spatial resolution is essential for effective treatment planning.⁽⁹⁾ CT is the primary imaging modality used for radiotherapy treatment planning. It helps to provide a detailed and accurate picture of the interested area⁽¹⁴⁾. On the other hand, CT

images offer both anatomical information and the electron density of internal tissues, which is essential for calculating dosage and optimizing treatment plans. A CT scanner is a device with a cylindrical opening and a platform on which the patient lies. The platform moves in the same direction as the patient's body inside the opening.

Furthermore, Magnetic Resonance Imaging (MRI) and Positron Emission Computed Tomography (PET-CT) are used for fusion, which enables a complete and comprehensive picture of the affected area ⁽¹²⁾.

2.1.2. SBRT in Treatment Planning

SBRT requires an initial preparation phase to plan for the treatment course. The planning phase involves a treatment simulation, referred to as the planning CT, which scans to identify and define the tumor and organs at risk (OARs) with a high degree of precision. The data obtained is then used to calculate and optimize the dose that will be administered to the patient over multiple treatment sessions to maximize the therapeutic effect and minimize the side effects. To ensure the reproducibility and accuracy of the treatment, the patient is positioned on the CT simulator couch in the same treatment position that will be used during the actual therapy. The medical team at the institution selects this specific position to ensure the patient's comfort and immobilization during the procedure. Additionally, permanent marks are placed on the patient's skin to indicate the tumor's location outside the body. These marks aid in guiding the positioning of the patient during treatment to ensure proper alignment between the treatment target and the isocenter of the linear accelerator.

SBRT is a specialized cancer treatment that directs radiation specifically to the tumor or affected area. This precise targeting makes it a highly effective treatment for certain types of cancer. However, the success of SBRT treatment depends on careful planning and adherence to the International Commission on Radiation Units and Measurements (ICRU) criteria. This includes considering factors such as ITV, PTV, margins, and OARs, all of which are crucial for ensuring accurate and efficient treatment. According to the ICRU 50/62/83, which is shown in the table,

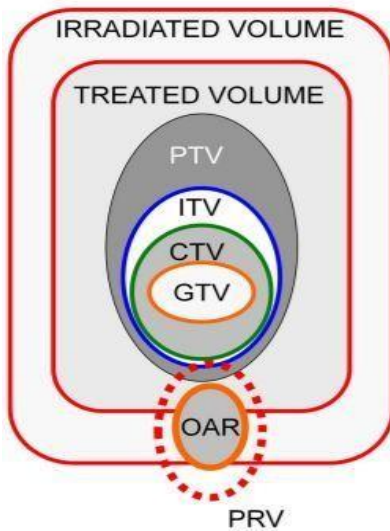


Figure 2.2. Schematic ICRU defined volumes and their relative sizes

- GTV: Gross tumor volume
- CTV: Clinical tumor volume
- ITV: Internal target volume
- PTV: Planning target volume
- OAR: Organs at risk
- PRV: Planning organ at risk volume

Gross tumor volume (GTV) refers to the visible tumor identified through imaging and clinical data. GTV acts as the initial reference point for treatment planning⁽¹⁵⁾.

Clinical Target Volume (CTV): This volume takes into consideration the possibility of undetected cancerous cells beyond the GTV. It is determined by factoring in an accommodation for the possibility of negligible tumor metastasis in addition to GTV. An Internal Margin (IM) is incorporated into the CTV to generate the ITV⁽¹⁵⁾.

Internal Target Volume (ITV): is a critical parameter that guarantees coverage throughout patient respiration and other internal movements. It considers the body's internal movements and variations in the CTV's dimensions, shape, and location.⁽¹⁶⁾.

SM (Set-up margin): Due to variations in patient positioning and the mechanical-dosimetric differences in devices, setup errors arising from human factors are measured separately for each field and each immobilization method and are planned in three dimensions⁽¹⁷⁾.

The ITV is calculated by adding the internal margin to the CTV, which is then expanded further by incorporating the setup margin to create the PTV.

The planning target volume (PTV) incorporates margins surrounding the ITV to account for changes in patient positioning and beam delivery. This assures that the prescribed dose is likely to cover the CTV⁽¹⁷⁾.

$$\text{PTV} = [\text{CTV} + \text{Internal Margin}] (\text{ITV}) + \text{Set-up Margin (SM)}$$

The Planning Organ at Risk Volume (PRV) includes all surrounding organs that are vulnerable to radiation and should be outlined as part of the treatment plan. Each of these organs has its own dose tolerance that must be considered during planning.

Isodose lines are chosen with a small or absent margin over the radiation penumbra at the planning target volume (PTV) edge to minimize dose drop and safeguard healthy tissues. In that way, dose heterogeneity within the target increases. Measuring and calculating the accurate dose becomes increasingly difficult as the target volumes get smaller. SBRT utilizes reduced field sizes, which demands precise beam modeling, including profiles and depth doses. Preferred over customized blocks, multileaf collimators (MLC) aid in beam shaping. Determining the MLC safety limit according to PTV creates hot spots that are desired to remain within the target without scattering to normal tissue. In addition, the MLC fiber width is taken as 5 mm⁽¹²⁾.

Ideally, the dose administered to the patient should be 95% compatible with the planned dose. To achieve this objective, radiation oncologists and physicians have access to various advanced radiation therapy techniques, each with unique strengths and applications. Through modern imaging techniques and advanced technologies like VMAT, IGRT, and adaptive radiotherapy, SBRT strives for the highest degree of precision in delivering radiation, thereby emphasizing the need for meticulous planning and execution in SBRT protocols. In conclusion, combining these advanced radiation therapy techniques can ensure that patients receive the best possible treatment.

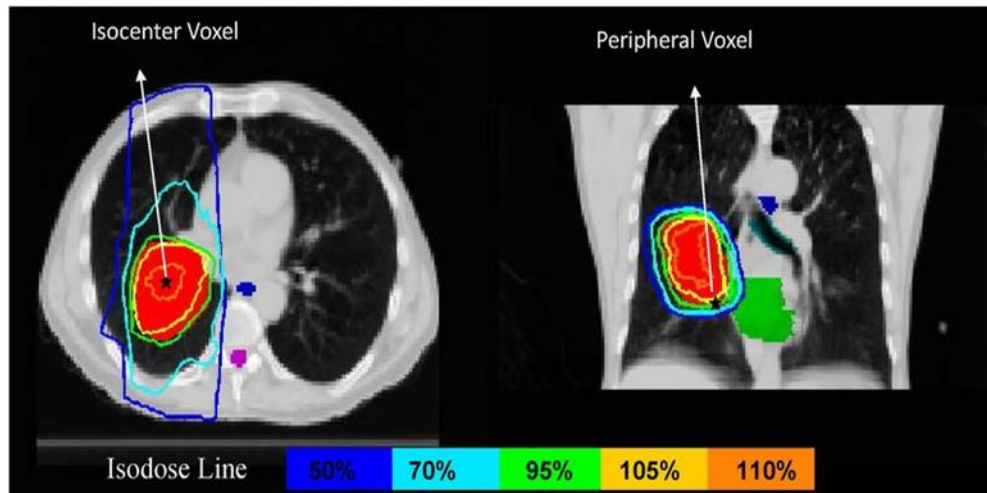


Figure 2.3. Isodose lines for a lung cancer patient are delineated for two separate voxels: isocenter and peripheral ⁽¹⁸⁾

2.2. Lung SBRT

Lung cancer has the highest death rate in the world among other cancer types. 80% of newly diagnosed cases of lung cancer each year are non-small cell lung cancer (NSCLC).

⁽¹¹⁾ The intricate movement of lung tumors, deeply intertwined with diaphragm motion and influenced by various factors such as tumor location, size, and disease stage, poses unique challenges in ensuring precise targeting during radiation therapy, especially in the context of NSCLC ⁽¹⁹⁾.

In lung SBRT, two significant problems are respiratory motion and tissue inhomogeneity ⁽¹²⁾. Due to tissue inhomogeneities, there are variations in the dose distribution in the lung environment, such as a decrease in absorption and an increase in lateral range. This can cause a charged particle imbalance and a buildup effect. Irregular and complex respiratory movement introduces several challenges in the precise planning and delivery of lung SBRT, impacting image quality and dose distribution. The key challenges include:

I. Variability in Motion: The extent and speed of respiratory motion vary significantly among patients, influencing the accuracy of tumor localization and radiation delivery. Furthermore, respiratory patterns can change during a single treatment session (intrafraction) and between different sessions (inter-fraction), presenting hurdles in maintaining consistent target coverage ⁽¹⁹⁾.

II. Imaging Artifacts: The acquisition time for individual slices in imaging modalities like CT, CBCT, MRI, and PET is only a fraction of a respiratory cycle, leading to potential artifacts that can obscure or distort the tumor and surrounding tissues⁽¹⁰⁾. These artifacts can result in distorted target volumes, leading to incorrect positional and volumetric information, which is crucial for accurate treatment planning.

III. Dose Distribution Concerns: Respiratory motion can introduce uncertainties in dose distribution while treating thoracic and abdominal lesions with particle beams, which can affect the efficacy of the treatment. The treatment planning process involves adding margins to the target volume to address the tumor motion. However, this approach is not ideal as it increases the radiation field size, exposing a larger volume of healthy tissue to high doses⁽²⁰⁾. Additionally, respiratory motion and potential changes in the tumor and normal tissues (shrinkage, growth, and shifts) due to radiation therapy or other treatments can vary daily, making it challenging to deliver consistent treatment⁽²⁰⁾.

Reducing the negative effects of respiratory motion and using advanced technologies to achieve better dose distribution and conformity has become increasingly crucial. SBRT technique has proved itself specifically in the early stage (T1-2 N0) of NSCLC to be as efficient as surgery⁽²¹⁾ and SBRT arises as a critical treatment option for individuals who are surgically unfit to fight lung cancer, a prevalent health issue on a global scale. Its favorable outcomes and safety profile provide renewed optimism for those affected by this malignancy. For lung SBRT, the dose reduction is more pronounced outside the target area. This is achieved by using small field sizes and non-coplanar radiation configurations, resulting in a dose distribution customized to the tumor's shape. Moreover, that is a suitable treatment option for metastatic lung cancers with small lesions⁽²¹⁾.

Clinical outcomes following SBRT for lung cancer have been a focal point of recent research, with studies demonstrating promising results in terms of local control and survival rates. SBRT with higher BED is now a standard treatment for early-stage NSCLC, achieving local control rates of over 90%⁽²²⁾. Patients treated with SBRT have observed two and 5-year cancer-specific survival rates of 94.6% and 80.0%, respectively⁽¹³⁾. A comprehensive review of 25 studies revealed that quality of life (QOL) remains consistent after SBRT in patients with early-stage non-small cell lung cancer⁽²³⁾. These findings underscore the

effectiveness of SBRT in managing early-stage NSCLC and its potential role in treating multifocal, recurrent, and oligometastatic disease.

In lung SBRT, 4-dimensional CT (4DCT) is used, which is more advantageous compared to 3D-CT and can record more than one image⁽¹⁶⁾. Thus, geometric errors that may occur due to position, shape, tumor, and volumes of normal structures are minimized in planning. Additionally, the movement of the tumor, healthy tissues, and organs associated with respiration varies on the patient's anatomical and physiological conditions, as well as the size and location of the tumor. The tumor can exhibit significant movements in all three dimensions: coronal, sagittal, and transverse. Considerable disparities arise between the intended and planned dosages due to this circumstance. PTV has been developed to mitigate uncertainties arising from respiratory motion, organ movements, and setup errors⁽¹⁶⁾.

2.2.1. Prescription for Lung SBRT Dose

SBRT is conducted based on specific protocols to ensure maximum efficacy and safety of the treatment. These protocols are designed by medical professionals and are based on dose limitations that are set after careful consideration of various factors, such as the size and location of the tumor, the patient's overall health and medical history, and the potential side effects of the treatment.

RTOG's Protocol: 0813

RTOG 0813 is a clinical trial aimed at treating patients with non-small cell lung cancer (NSCLC) in its early stages that is located centrally and cannot be operated on. The study included patients who had T1-2, N0, or M0 non-small cell lung cancer (tumor diameter ≤ 5 cm) and had the disease contiguous to the pericardial or mediastinal pleura. It was affected by or in the proximal bronchial tree region⁽²⁴⁾. The treatment course is intended to be delivered over 1.5 to 2 weeks in 5 fractions, administered twice to three times weekly.²⁷ The treatment doses will be administered as follows: 8 Gy, 8.5 Gy, 9 Gy, 9.5 Gy, 10 Gy, 10.5 Gy, 11 Gy, 11.5 Gy, and 12 Gy⁽²⁴⁾.

RTOG's Protocol: 0915

The RTOG 0915 protocol was initiated as a phase 2 trial for patients with early-stage, medically inoperable, non-small cell lung cancer (NSCLC) in peripheral lung lesions. The study was focused on patients with tumors that were settled in peripherally located areas and had negative PET nodes (> 2 cm in all directions to the proximal bronchial tree) and early

phases of non-small cell lung cancer (T1, T2; less than 5 cm) that were medically inoperable. ⁽²⁵⁾ The treatment plan consisted of two arms of progressive treatment doses (1 fraction x 34 Gy and 4 fractions x 12 Gy) which had to be completed for four consecutive days ⁽²⁵⁾. Between fractions, a minimum of 18 hours must elapse, and determining the treatment period is at the researcher's discretion ⁽²⁵⁾.

– **Dosimeter for 0813 and 0915**

95% of the PTV should take the full prescription isodose, and 99% of PTV must take 90% of the prescription dose.

High Dosage Area: Doses greater than 105 % of the prescription dose should be mainly within PTV and not in normal tissues other than PTV. Therefore, the cumulative volume of all tissues receiving more than 105 % of the prescription dose except PTV should not exceed 15% of the volume of PTV.

Low-Dose Area: After PTV, normal tissue doses should be kept relatively low, with a sharp decrease in dose. The following table shows the criteria for evaluating the treatment plan's quality based on the tumor's diameter.

Table 2.1. Prescription dosage conformity in heterogeneous tissues for photon ⁽²⁵⁾

PTV Volume (cc)	Ratio of Prescription Isodose Volume to the PTV Volume		Ratio of 50% Prescription Isodose Volume to the PTV Volume, R _{50%}		Maximum Dose (in % of dose prescribed) @ 2 cm from PTV in Any Direction, D _{2cm} (%)		Percent of Lung Receiving 20 Gy Total or More, V ₂₀ (%)	
	Deviation		Deviation		Deviation		Deviation	
	None	Minor	None	Minor	None	Minor	None	Minor
1.8	<1.2	<1.5	<5.9	<7.5	<50.0	<57.0	<10	<15
3.8	<1.2	<1.5	<5.5	<6.5	<50.0	<57.0	<10	<15
7.4	<1.2	<1.5	<5.1	<6.0	<50.0	<58.0	<10	<15
13.2	<1.2	<1.5	<4.7	<5.8	<50.0	<58.0	<10	<15
22.0	<1.2	<1.5	<4.5	<5.5	<54.0	<63.0	<10	<15
34.0	<1.2	<1.5	<4.3	<5.3	<58.0	<68.0	<10	<15
50.0	<1.2	<1.5	<4.0	<5.0	<62.0	<77.0	<10	<15
70.0	<1.2	<1.5	<3.5	<4.8	<66.0	<86.0	<10	<15
95.0	<1.2	<1.5	<3.3	<4.4	<70.0	<89.0	<10	<15
126.0	<1.2	<1.5	<3.1	<4.0	<73.0	<91.0	<10	<15
163.0	<1.2	<1.5	<2.9	<3.7	<77.0	<94.0	<10	<15

These protocols require that they correct tissue heterogeneity for monitor unit calculation and dose planning in actual treatments. Certain algorithms approved by the RTOG Physics Committee should be used in dosage calculations. According to these protocols, the superposition/convolution dosage calculation algorithms match the planned and applied doses. Other than this, the accuracy of other algorithms must be demonstrated by various methods.

2.2.2. Immobilization in Lung SBRT

In lung SBRT applications requiring narrow PTV margins, the major challenge is to accurately determine the tumor's location and ensure precise targeting of radiation beams. This is because the tumor and surrounding tissues can shift position due to irregular respiratory motion. Moreover, these movements can vary depending on the size and location of the tumor. For instance, smaller tumors and those located near the lower lobe or diaphragm tend to move more. Considering all these factors, choosing an immobilization device tailored to the individual patient and tumor is crucial.

Many devices, such as vacuum bags, wing boards, T-bars, knee cushions, and body fixes, are used to immobilize the lung during SBRT. Techniques such as abdominal compression and active breath-holding can also help keep the tumor in place during treatment. Various techniques, such as image guidance, tumor tracking, and respiratory gating, have been developed to address lung motion during treatment.



Figure 2.4. Commercially available immobilization devices

2.2.3. Strategies for Respiratory Motion Management

Multiple strategies for managing respiratory motion are designed to deal with particular problems caused by tumor growth and patient movement during the breathing cycle. The main strategies consist of:

Table 2.2. Comparative Overview of Strategies

Strategy	Key Feature	Application
Motion Encompassment	Covers the full range of tumor motion	Used when tumor motion is predictable and well-defined ⁽²⁰⁾ , most frequently employed while using SBRT to treat central lesions ⁽²⁶⁾
Respiratory Gating	Synchronizes radiation delivery with respiratory cycle	Ideal for tumors with a stable position during certain respiratory phases ⁽¹⁹⁾
Breath-Hold	Reduces tumor motion by pausing respiration	Suitable for patients who can consistently hold their breath for short periods
Motion Mitigation	Reduces the effect of respiratory motion on tumor position	Applied when normal breathing needs to be maintained without significant tumor movement
Tumor Tracking	Adjusts radiation beam in real-time to follow tumor movement	Recommended for tumors with unpredictable or extensive movement

The choice among these strategies depends on various factors, including the tumor's location, the patient's respiratory stability, and the available technology. For instance, breath-hold may become a standard practice to reduce pulmonary and cardiac toxicity in breast irradiation, highlighting the significance of motion management in lung SBRT and treatments involving other thoracic and abdominal organs⁽²⁰⁾. Furthermore, the integration of image-guided respiratory motion management has been identified as crucial in modern radiotherapy, underscoring the importance of advanced imaging techniques in enhancing treatment precision.

2.2.4. Tumor Motion Definition with Imaging in Lung SBRT

Precisely determining the precise location and size of the tumor is a crucial element in the process of planning treatment in radiotherapy. This is crucial because one of the primary objectives in treatment planning is to protect the organs at risk (OAR) while administering the prescribed dose to the tumor. The thoracic and abdominal regions pose significant challenges in accurately delineating the tumor volume. The primary factor is that tumors located in those two regions experience the most significant movement due to respiration. The patient's movement and breathing can cause motion in three separate directions: anterior-posterior (AP), superior-inferior (SI), and left-right (LR). Among these, the dominant direction of tumor motion is usually superior and inferior.

It's crucial to accurately estimate the mean position and range of motion during CT imaging. This is because tumor motion induced by respiration during radiation therapy can affect the outcome. When using imaging techniques involving respiration, it's essential to adhere strictly to radiation dose compared to standard CT simulation images⁽²⁰⁾. Many methods in radiotherapy can cover respiratory movement fully. They are:

A. Slow CT

The use of slow CT technology is particularly effective in planning treatment for tumors that are prone to movement, such as those found in the upper abdomen or peripheral lungs⁽²⁰⁾. These tumors can shift due to natural bodily functions like breathing or digestion, making it challenging to administer precise radiation doses using traditional imaging techniques. Unlike conventional CT scans, slow CT captures multiple images over several breathing cycles, offering a more comprehensive view of the tumor and surrounding tissues⁽²⁷⁾. These images are then merged to create a detailed image of the tumor's movements and surrounding tissues, enabling personalized and more effective radiotherapy treatment plans. Slow CT can help diagnose small lesions or subtle abnormalities that may not be readily apparent on a standard CT scan.

This technology helps minimize the impact on healthy tissues surrounding the tumor, ensuring more precise targeting of the radiation dose. However, it's essential to note that this approach has limitations, including uncertainty about the tumor's exact size and shape and blurring of the surrounding anatomy⁽²⁷⁾. As a result, slow CT scans are primarily recommended for lung tumors that don't interact with the chest wall or mediastinum⁽²⁰⁾.

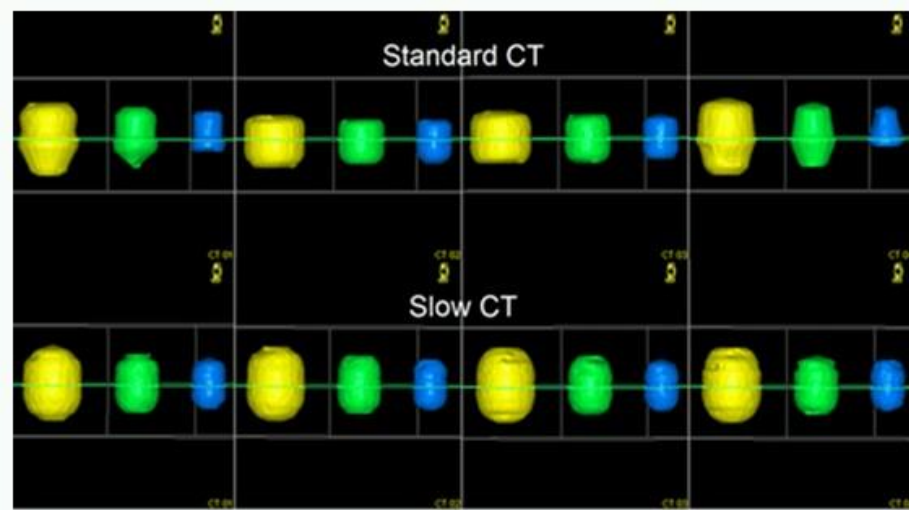


Figure 2.5. Comparison between Standard and Slow CT in peak-to-trough motion of 1.5 cm for 4 images ⁽²⁷⁾

B. Inhale-Exhale position breath-hold CT

The inhale-exhale breath-hold CT technique is a diagnostic method used to capture CT scans at two different phases of a patient's breathing cycle: full inhalation and full exhalation. This technique is beneficial for identifying the volume that encompasses lung tumor motion through accurate fusion and MIP formation ⁽²⁰⁾. The captured images are used to create a clear view of the anatomy. MIP can highlight areas of high contrast, such as tumors or vascular structures, making it easier to identify them amidst dynamic changes during inhalation and exhalation. However, this method is only suitable for patients who can hold their breath throughout the entire CT scanning process, as both inhaling and exhaling must be captured. The dynamic changes in the anatomy during inhalation and exhalation can create challenges in image interpretation. Image fusion can integrate inhale-exhale position CT images with other modalities like MRI or PET to provide a more detailed view of the anatomy. Additionally, this technique has better resolution compared to slow CT.

C. Four Dimension Computer Tomography (4DCT)

4DCT is a vital tool in respiratory motion management. The fourth element is "time". Unlike CT scans that create detailed three-dimensional images of tumors, organs, and tissues,

the 4D images obtained in 4DCT consist of scans acquired from each respiratory phase of the breathing cycle. 4D CT imaging presents several benefits in comparison to conventional CT imaging. The utilization of 4DCT facilitates the creation of phase-resolved reconstructions, which enhance the accuracy of tumor targeting in radiation therapy. Data is collected by adding the time required for single image reconstruction to the duration of one respiratory cycle. The result is then examined to determine whether the data sufficiency condition (DSC) is met ⁽²⁸⁾. While the 4DCT image may superficially resemble the "cine" of a solitary composite respiratory cycle, it comprises ten distinct respiratory phases ⁽²⁹⁾.

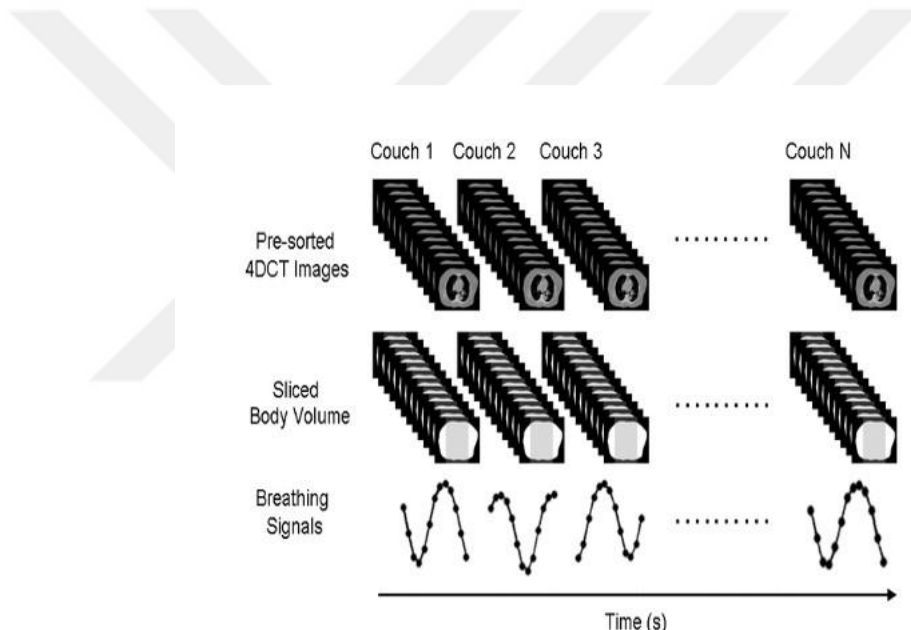


Figure 2.6. An illustration of how individual image slices are transformed into a 4DCT image using the respiratory signal.

4DCT is a commonly used imaging technique for lung cancer patients undergoing SBRT treatment. This technique helps provide a better understanding of the target motion in moving targets, making it easier for clinicians to approach radiation therapy. It is also known as 'dynamic volumetric imaging' or 'respiration-correlated CT' and has significantly improved how medical professionals approach radiation therapy. Understanding the nuances of 4DCT

scan and 4DCT radiation therapy, including its advantages and challenges, is essential for maximizing its benefits in treating lung cancer.

– **Advantages of 4DCT in Lung SBRT**

Clinical trials utilizing 4DCT in lung SBRT have demonstrated several significant.

1. Enhanced Visualization and Accuracy:

- Enhanced visualization of moving targets, such as lung tumors, is crucial for precise treatment planning and delivery accuracy⁽³⁰⁾. Improved temporal resolution facilitates this visualization, providing clearer insights into the dynamic nature of tumor movement over time.
- Real-time tracking of tumor motion enables clinicians to precisely target the tumor during radiation therapy. Continuously monitoring tumor movement can make treatment adjustments in real-time to ensure optimal targeting. This real-time tracking also allows for selecting the most stable phase of the respiratory cycle for each patient, improving the accuracy of treatment delivery.⁽³¹⁾

2. Reduced Radiation Exposure:

- One significant benefit of advanced techniques in radiation therapy is the potential for reduced radiation exposure to healthy tissues, thereby enhancing the overall safety of the treatment process⁽³⁰⁾. By utilizing innovative approaches, clinicians can better target tumors while minimizing radiation exposure to surrounding healthy tissues.
- Studies comparing 4DCT-based treatment plans with traditional 3DCT-based plans have demonstrated superior sparing of normal tissues, particularly in early-stage lung cancer radiotherapy.⁽³²⁾

3. Reduced Planning Target Margins: By simultaneously enabling patient-individual motion assessment and safety margin adjustment, 4DCT effectively mitigates motion artifacts, thereby facilitating precise delineation of target volumes.⁽³³⁾

- **Motion Management:** 4DCT-informed motion management effectively reduces ITV-based margin expansion, minimizing the need for envelope-based margin expansion based on conventional 3DCT scans. Studies have demonstrated that 4DCT improves the quality and robustness of plans, particularly when setup uncertainties are 3, 4, and 5 mm. This

results in reduced average values for D95%, D98%, and D99% in comparison to PTV-based optimization.⁽³⁴⁾

- **Patient-Specific Reduction:** 4DCT imaging has the capability to generate individualized internal target volumes (ITV).

Multiple techniques are used to ascertain the target volume. A rapid method is to generate ITV from 4DCT datasets using MIP, AIP, and Min IP. These projections are generated as composite images by aggregating the phases of tumor positions that occur during each respiratory phase. As a result, they directly facilitate the establishment of ITV.

MIP (Maximum Intensity Projection): 4DCT utilizes MIP for target contouring and treatment planning in the context of lung cancer. It evaluates voxels in four dimensions and selects them according to their maximum CT values when creating a new volume. It enables the creation of ITV quickly and accurately.

Min IP (Minimum Intensity Projection): It evaluates voxels in four dimensions and selects them according to their minimum CT values when creating a new volume.

AIP (Average Intensity Projection): It is used to determine the location where the tumor is most prevalent throughout the respiratory cycle.

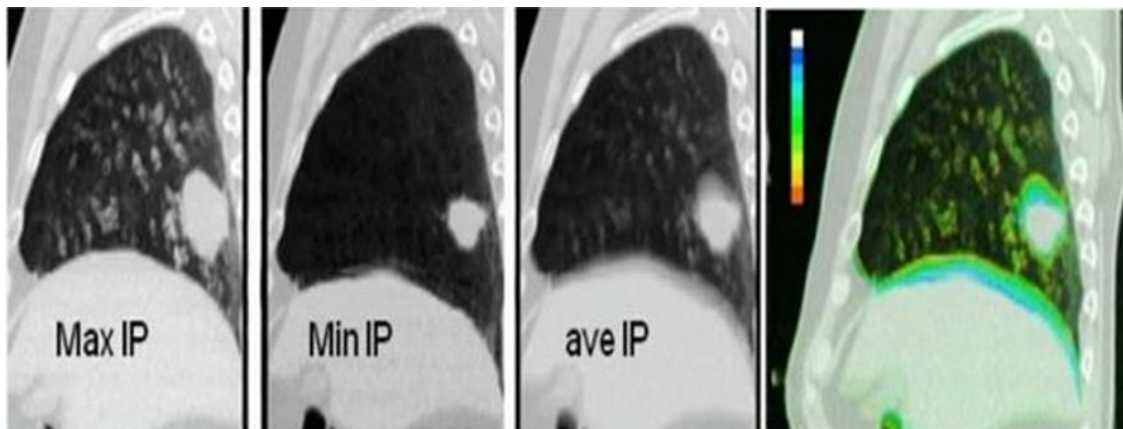


Figure 2.7. MIP, Min IP, AIP of a lung tumor.

For lung tumors, the usual approach is to utilize maximum intensity projection (MIP) to delineate the tumor throughout all phases of the respiratory cycle (typically, 10 phases) and thereby generate the internal target volume (ITV).⁽³⁵⁾ In the presence of respiratory movement, it can acquire high-quality CT data. The lung parenchyma is more clearly visible when utilizing MIP images.

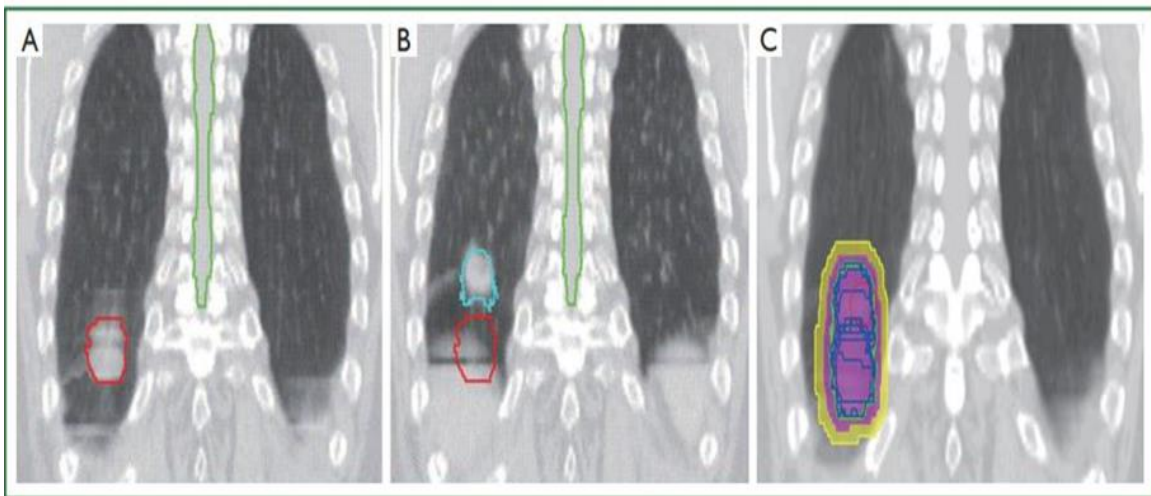


Figure 2.8. An early-stage lung cancer patient's 4DCT images at end-inhalation (A) and end-exhalation (B), along with combined outlines from all 10 4DCT phases (C) is displayed⁽³⁴⁾

- Disadvantages of 4DCT in Lung SBRT

While 4DCT provides significant advantages in lung SBRT, it also presents several disadvantages that merit consideration:

Image Artifacts and Local Control: 4DCT image artifacts correlate with worse local control in SBRT for lung and liver metastases, suggesting that these artifacts could negatively impact treatment outcomes. Enhancing image quality is crucial for reducing delineation uncertainty.

Breathing Irregularities and Motion Artifacts: 4DCT techniques can assume irregular breathing patterns, which can be problematic. Such patterns can cause data acquisition and respiratory phases to mismatch, leading to motion artifacts and potentially compromising the accuracy of 4DCT imaging⁽³⁶⁾. These challenges underscore the importance of implementing alternative techniques or mitigation strategies to address breathing irregularities. Various approaches have been proposed, including respiratory coaching, gating, and post-processing techniques, all of which aim to minimize motion artifacts⁽³⁶⁾.

Challenges in Treatment Planning: Distinguishing between tumor and surrounding tissue can be difficult when utilizing techniques like MIP, as they tend to overestimate the size of the PTV⁽³⁶⁾. A recent study has revealed that the geometrical diversity of tumors located in lower lobes and adhered to chest walls and diaphragms pose a significant challenge. This is further emphasized by the statistical distinction in D98% PTV⁽³⁷⁾.

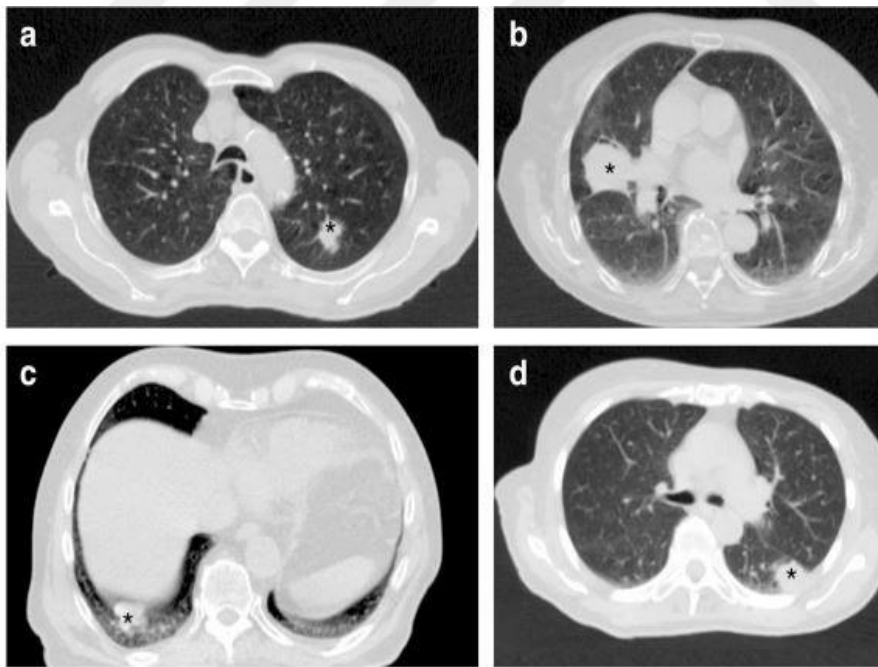


Figure 2.9. The sequences a, b, c, and d depict lung tissue, metastasis, diaphragm, and chest wall in the lung cancer images⁽³⁵⁾

In conclusion, reconstructed MIP images may incorrectly misclassify the ITV in instances of substantial irregular breathing patterns or when tumors lie adjacent to structures of soft tissues (such as the diaphragm, chest wall and mediastinum). In such cases, MIP ought to be utilized judiciously, and the design of the ITV should account for each of the ten respiratory phases. Then, a person-specific PTV is created by giving a 5mm margin to ITV. (37)

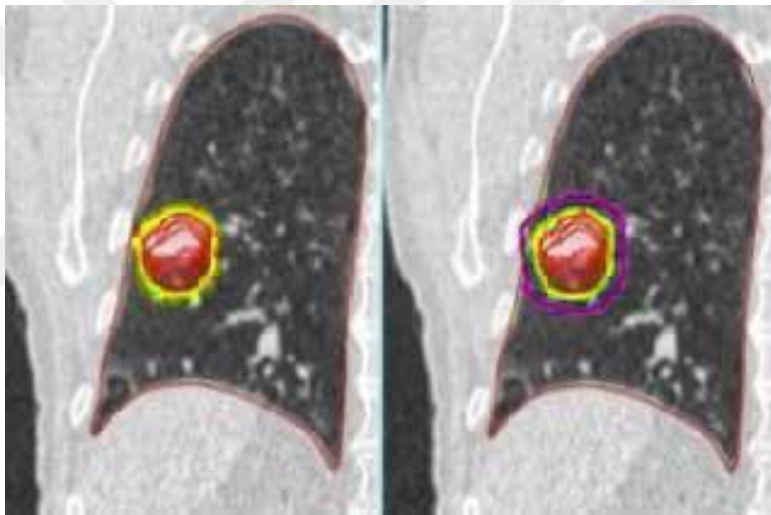


Figure 2.10. ITV (yellow) and PTV (purple) volumes obtained by adding 5mm to the ITV.

2.2.5. Implementing Advanced Techniques in Motion Management for Lung SBRT

Respiratory motion, a patient-specific characteristic that varies in period, amplitude, and regularity, plays a significant role in the motion management of lung SBRT. ⁽¹⁰⁾ Given the critical need for accuracy in targeting the tumor while minimizing dose exposure to surrounding vital organs, motion management in lung SBRT has emerged as a keystone in optimizing treatment outcomes. This encompasses a variety of strategies, including breath-holding, respiratory gating, tumor tracking, abdominal compression, internal target volume (ITV), and mid-ventilation (Mid-V) scan, each tailored to accommodate each patient's unique respiratory cycle ^(19,36)

Table 2.3. Comparative Analysis of Techniques

Technique	Advantages	Disadvantages
DIBH	Reduces PTV margins and dose, improves tumor control	Requires patient cooperation, trained therapists for coaching ⁽²⁰⁾
Respiratory Gating	Aligns radiation with respiratory cycle, optimizing targeting	It needs synchronization with the patient's breathing external devices ⁽³⁸⁾
Tumor Tracking	Real-time tumor localization adjusts radiation delivery	Increases treatment complexity, requires advanced imaging ⁽⁹⁾
Only ITV	Incorporating respiratory motion, Improved coverage of targets, The quality of adaptability	Complexity in treatment planning, Increased Treatment Volume
Abdominal Compression	Reduces the effect of respiratory motion on tumor position	Discomfort as a result of respiratory restriction, Distortion in imaging in the abdominal or pelvic region.

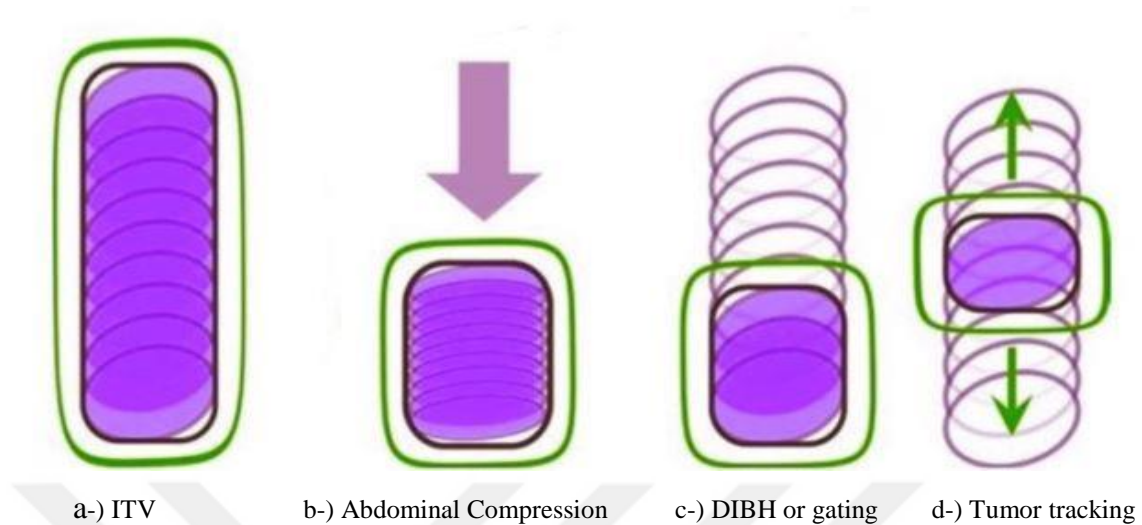


Figure 2.11. Comparison Between (a) ITV, (b) Abdominal Compression, (c) DIBH or Gating, and (d) Tumor Tracking.

2.2.5.1. Breath-Hold Radiotherapy Techniques

a) Deep Inspiration Breath Hold (DIBH):

Using this method, the patient inhales deeply during radiation treatment. DIBH expands healthy lung tissue and immobilizes the tumor, reducing PTV margins and lung dose compared to traditional ITV-based radiation therapy in free-breathing scenarios ⁽⁹⁾. The process can be voluntary or computer-controlled with the assistance of spirometry or surface-based systems, making it easier for the patient to cooperate during the procedure.

b) Active Breathing Control (ABC)

Elekta employs the ABC technique, which facilitates measurable and consistent breath-holds. The ABC apparatus is frequently employed during moderate or profound inhalations and can halt respiration in any predetermined position ⁽³⁹⁾. The apparatus comprises a digital spirometer that is linked to a balloon valve to quantify the respiratory trace. A routine inhalation is taken by the patient through the apparatus throughout an ABC procedure. When the operator "activates" the system, terms pertaining to the lung volume and the respiratory cycle phase during which the inflated valve will retract are specified. The patient is then instructed to attain the specified lung volume, which is typically accomplished after two pre-exhalatory breaths have been completed. The valve is then inflated with an air compressor for a predetermined period of time, effectively "holding" the patient's breath. The breath-hold duration is patient-specific and typically ranges from 15 to 30 seconds ⁽²⁰⁾. It is

crucial that the patient can tolerate repeated breath-holds (after a brief interval of rest) without experiencing undue distress.

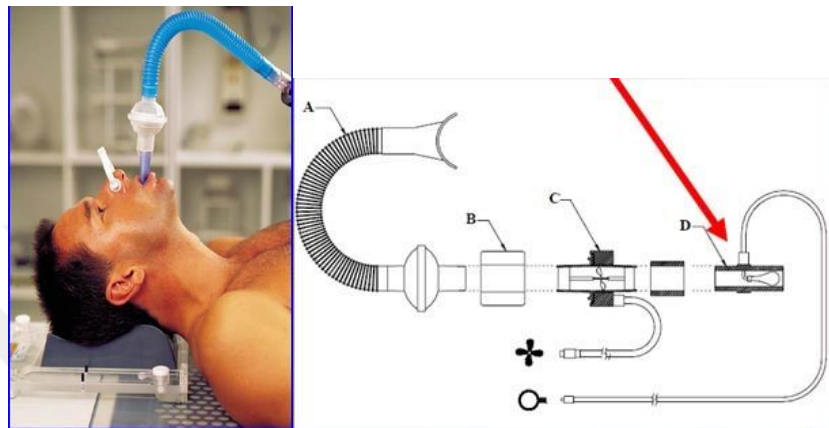


Figure 2.12. Spirometer, Active breath-holding

To optimize the CT scan, it's important to consider the maximum time a person can hold their breath without moving. This is especially important when applying contrast during the scan of the area of interest. Based on the intended verification strategy, a margin will be added to treatment plans. By using breath-hold techniques instead of unrestricted breathing, the GTV margins can be reduced, which helps to protect the lungs.

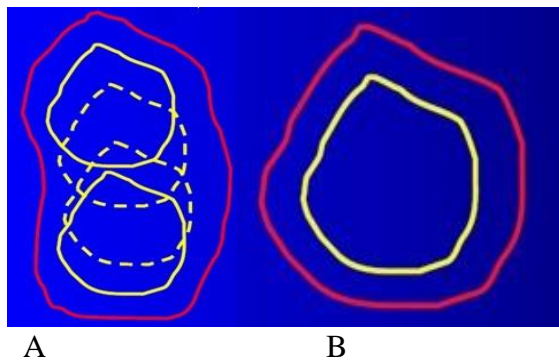


Figure 2.13. Free breathing(A) and breath hold(B) GTV margins

c) **Abdominal Compression (AC)**

The application of forced shallow respiration with abdominal compression has been limited to the treatment of early-stage lung tumors that do not involve the mediastinum or have nodal disease. A stereotactic body frame with an attached plate that is placed against the abdomen is utilized in this method, in which the tumor motion exceeds 5mm⁽²⁰⁾. The plate's angled sides are situated at a distance of 2 to 3 centimeters below the triangular rib cage⁽²⁰⁾. Typically, the greatest pressure that the patient can tolerate comfortably throughout the duration of the treatment session is applied. While imposing abdominal pressure, diaphragmatic excursions are diminished, allowing for a restricted degree of regular respiration.



Figure 2.14. Abdominal Compression

2.2.5.2. Respiratory Gating Treatment Techniques

Another frequently employed technique in the clinic is known as Gating. Gating involves administering the treatment (activating the radiation beam) exclusively when the patient is at a specific breathing phase or within a specific range of breathing phases, as determined during the planning process. Respiratory gating is a technique used to improve the accuracy of radiation therapy by aligning the delivery of treatment or image acquisition with the patient's respiratory cycle. It involves a trigger mechanism that activates and deactivates treatment delivery or image acquisition based on the tumor's position, ensuring

optimal targeting. However, this technique requires synchronization with the patient's breathing pattern, which is often achieved using external devices to predict the phase of the breathing cycle while the patient breathes freely. Two distinct forms of gating are employed.

A. External Respiratory Signal Tracking Treatment

Varian Real-time Position Management™ (RPM) system, BrainLab ExacTrac Gating/Novalis Gating®, Siemens Medical Systems Anzai belt radiotherapy centers are commercial systems used.

In radiation oncology, the Varian RPM system is a prevalent instrument that facilitates the visualization of the tumor's movement during the patient's respiration and provides accurate images of the target for radiation therapy. A marker block is applied to the patient, and an infrared surveillance camera is utilized by RPM to establish a correlation between the tumor's location and the patient's respiratory period. RPM with patient position tracking: by monitoring the position of the marker block in 3 dimensions (vertical, longitudinal, oscillating), it detects unexpected movement of the mark block in any direction. The restraint bars are modified to correspond with the particular phase of the respiratory period where the tumor is situated once the motion pattern of the tumor is discerned in relation to the wave shape. These patterns dictate when the automatic limitation procedure will take place using the "healing beam" and "cutting off the healing beam" instructions. The patient has normal respiration during the course of treatment. By concentrating his efforts on the treatment margin that pertains to patients, he achieves the simultaneous objective of increasing the dosage prescribed for the tumor and decreasing the dosage administered to the adjacent tissues. 4DCT data acquisition has two modes: prospective and retrospective gating. *Retrospective:* A continuous image is taken at each table position. It associates the images taken with the time pattern of the breath.

Prospective: Images are taken at specified phases of respiration

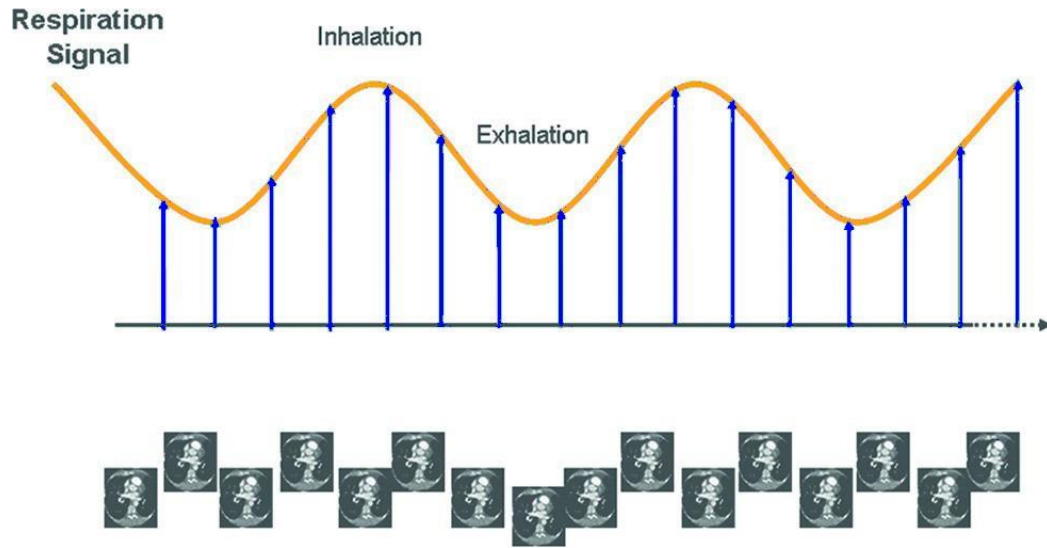


Figure 2.15. Retrospective gating for 4D CT data acquisition

B. Internal Respiratory Signal Tracking Treatment

Fiducial Marker: Radiotherapy utilizes systems that monitor tumors in real-time. 2-4 mm in diameter golden spherical markers are positioned inside or close to the tumor. The marker position's three-dimensional monitoring is achieved by acquiring stereotactic kV X-ray image pairs at various rates per second.

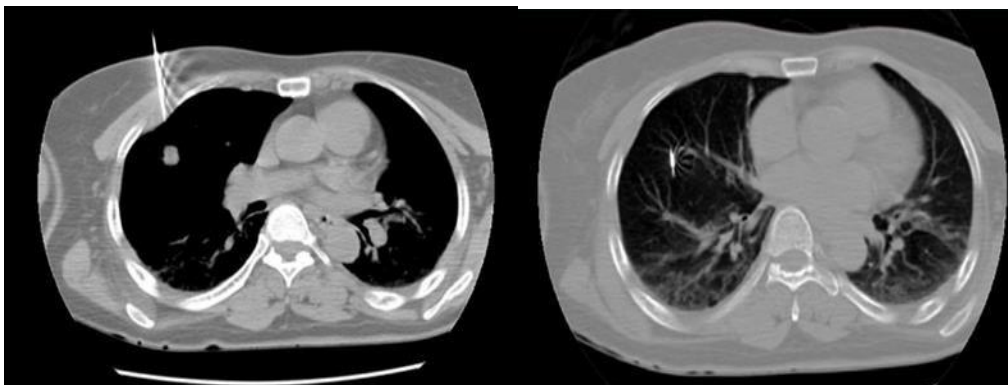


Figure 2.16. Fiducial markers in internal and external movement

2.3. IMAGE GUIDED RADIATION THERAPY (IGRT)

As medical science continues to evolve, advanced radiation therapy techniques such as SBRT, SRS, IMRT, and VMAT have been developed and are now being used together. This is because they offer a range of benefits, including a decrease in the planning target volume (PTV) margins allocated to the target volume. This reduction in the PTV margins means that the radiation therapy beam is more focused, which can increase the efficacy of the treatment. However, since the patient is being exposed to an ionization beam, it is critical to ensure that the planned and delivered doses are identical. Otherwise, major errors may occur, which could compromise the patient's safety and well-being. The Image-Guided Radiation Therapy (IGRT) method has been developed to address this issue. The precision and efficacy of sophisticated radiotherapy methods, such as SBRT, heavily depend on using image guidance before and during treatment.

Research has shown that IGRT is particularly crucial for improving the accuracy of treatment for moving tumors such as lung cancer. By using this method, physicians can adjust the radiation therapy beam to ensure that it is precisely targeting the tumor at all times, no matter how much it moves during the session. This level of precision can increase the effectiveness of the treatment while minimizing the risk of side effects. In general, IGRT is an indispensable component of modern radiation therapy and is continuously enhancing patient outcomes.

Image-guided radiation therapy (IGRT) is not a radiotherapy technique; it is a control process that verifies the treatment technique and area in each radiotherapy session. It compares pre-treatment, intra-treatment, and post-treatment images, taking into account setup errors and inter-fraction organ movements⁽⁴⁰⁾. IGRT Tools are PET/CT, MRI, 4D-CT for treatment planning and Ultrasound, Kilovoltage Cone-Beam CT, Megavoltage Cone-Beam CT, Helical Tomo-therapy, and immobilization for treatment delivery⁽⁴¹⁾.

IGRT Advantages in the radiotherapy:

- Considering setup errors improves tumor tracking.
- Adapting to changes in anatomy, such as tumor shrinkage or patient weight loss, makes precision radiation delivery to the intended target possible.
- Achieving a high dose of radiation precisely on the tumor ensures high precision in treatment by minimizing radiation exposure to healthy tissues and organs.

- It enables treatment with smaller treatment margins.
- Verify the treatment technique and the treatment application sites during each session to ensure the secure completion of the treatment.
- By utilizing advanced imaging technologies, it describes normal and tumorous structures before treatment and administers therapy with extreme accuracy and precision.

To meet these requirements, imaging devices mounted in the treatment room or directly on the Linac machine are utilized. Modern Linacs have two types of imaging systems.

- **kV portal imaging:** This technique consists of a kilovoltage X-ray tube and a flat panel detector directly opposite it. It provides 2D, 3D, and 4D imaging. Imaging techniques such as radiography, fluoroscopy, and 4DCBCT have this capability.
- **MV portal imaging:** which features an electronic portal imaging device (EPID) mounted directly opposite the gantry. Provides 2D and 3D imaging.

Elekta and Varian manufacturers have developed imaging systems named XVI and OBI, respectively. These systems are mounted on retractable arms that can rotate 90 degrees around the LINAC's central axis, providing KV CBCT capabilities ⁽⁴²⁾. Additionally, Siemens offers KV and MV CBCT systems.

2.3.1. Cone beam CT (CBCT)

Cone Beam Computed Tomography (CBCT) is a type of medical imaging that creates detailed 3-dimensional images of bones and soft tissues inside the body ⁽⁴³⁾. Unlike conventional medical CT scans (which employ a fan-shaped X-ray), CBCT uses a cone-shaped X-ray source and a detector to produce multiplanar projections of a patient in a single rotation.

kV CBCT: involves acquiring multiplanar projection images in many directions with a gantry rotation of 180 degrees or more.

MV CBCT: multiplanar projection images are obtained as the gantry and detector rotate around the patient.

Rotating in the x-ray gantry obtains 3-dimensional volumetric images by reconstructing these projections with a computer algorithm ⁽⁴⁰⁾. This helps in better visualization and understanding of the tumor's location and shape, allowing for more accurate treatment planning. With CBCT, complex conditions such as weight loss and the shape or

volume of the patient's tumor can be monitored. In this way, changes in the target position are corrected before treatment.

KV CBCT images are more compatible with reference treatment plan images than MV CBCTs for patient setup verification and correction⁽⁴⁴⁾. Also, kV CBCTs offer higher contrast visibility and spatial resolution for soft tissues than MV CBCTs⁽⁴²⁾. The typical resolution of a KV CBCT at the isocenter is approximately 1mm voxel size. In contrast, MV CBCT has a lower contrast of soft tissues but is good enough to verify the target position relative to the surrounding bony structures or fiducials.

However, it is important to note that CBCT does not provide images of the same high quality as the conventional fan-beam CT⁽⁴⁴⁾. This is due to the technique used to generate the images, which results in blurring. In studies conducted on the use of 3D CBCT for imaging the lungs, it has been found that this technique can result in blurring and diaphragm artifacts in a single 3D image generated from average projections obtained from respiratory phases⁽⁴⁰⁾. The blurring and artifacts in the generated images can cause inaccurate tumor location and size identification, resulting in incorrect treatment planning. Inaccurate treatment planning can lead to radiation damage to healthy tissues surrounding the tumor, which can cause long-term health problems for the patient.

2.3.2. Four-dimensional Cone Beam Computed Tomography (4DCBCT)

4DCBCT is an innovative imaging method that incorporates time as the fourth dimension, providing a sequence of three-dimensional images that illustrate changes over time. This technology enables the visualization of tumor movements during treatment, allowing for more accurate radiation delivery and sparing healthy tissues from unnecessary exposure. The modality stands out with higher image quality, real-time imaging capabilities, and a broader range of clinical applications compared to other imaging options.

In 4DCBCT, imaging is conducted across multiple respiratory phases. This means several images are taken while the patient breathes at different respiratory cycle phases. Each projection represents a different respiratory phase, allowing for a more comprehensive view of the area being imaged⁽⁴⁵⁾. To create a 4D image, the projection images are classified based on the respiratory signal and reconstructed into subsets⁽⁴⁶⁾. This process generates a 4D image that shows the area of interest at different respiratory phases⁽⁴⁶⁾.

For each breathing cycle, the image that is in closest proximity to each respiration phase is chosen⁽⁴⁵⁾. This helps to ensure that the image accurately reflects the area of interest at that specific respiratory phase.

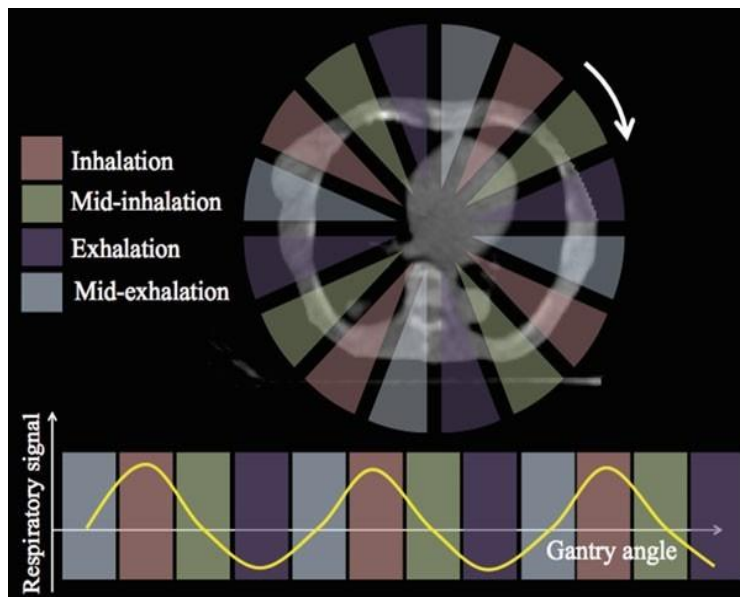


Figure 2.17. The reconstruction principle of 4DCBCT involves using projections acquired from 4 respiratory phases⁽⁴⁶⁾

Managing respiratory motion is crucial in high-precision external radiotherapy⁽⁴⁷⁾. While 3DCBCT can only provide static images, 4DCBCT offers dynamic images that showcase the motion of tumors and organs. By accounting for internal movements caused by breathing, 4DCBCT reduces uncertainties in tumor positioning, leading to more accurate image-guided radiation therapy⁽⁴⁸⁾. The 4DCBCT technology has proven effective in monitoring dynamic changes in lung function during radiotherapy. It has allowed real-time monitoring and potential adjustments in treatment plans aimed at minimizing radiation dose. Particularly beneficial for imaging isolated tumors or those near the diaphragm, 4DCBCT's

grayscale registration allows for effective mean density projection⁽⁴⁹⁾. The technology aids in establishing consistent protocols across lung cancer radiotherapy, promoting uniformity in treatment approaches, and ensuring precise setup correction, which is essential for accurate tumor localization⁽⁴⁹⁾. 4DCBCT offers significant advantages over 3DCBCT in terms of more precise localization of moving targets, alleviation of structural blurring, motion tracking, and facilitation of adaptive radiation therapy⁽⁵⁰⁾.

For SBRT targeting lung tumors, 4DCBCT is the preferred volumetric image guidance technology, indicating its reliability in clinical settings⁽³³⁾. PTV is determined by considering tumor movement, which depends on respiration with 4DCBCT in lung SBRT⁽⁹⁾. Moreover, to improve the precision and accuracy of dose delivery, a registration process is performed between the 4DCT planning and 4DCBCT⁽⁴⁷⁾. This process involves aligning and comparing the two images to verify and correct tumor motion, ensure that the radiation is delivered accurately to the tumor, and minimize damage to surrounding healthy tissues.

The 4DCBCT technology also enables precise evaluation of both inter-fractional and intra-fractional variations in tumor position and shape before target irradiation⁽⁵¹⁾. Its capabilities in detecting even the smallest changes in tumor position and shape are unparalleled, making it a valuable asset in cancer treatment plans. With the ability to verify the mean position, trajectory, and shape of a tumor within the treatment, 4DCBCT is particularly effective in minimizing the uncertainties caused by respiration for moving targets⁽⁵²⁾. This is a crucial factor in ensuring the accuracy of radiation therapy, as even the slightest changes in tumor position or shape can significantly impact treatment outcomes. In comparison to 3DCBCT images, which may miss small changes, 4DCBCT offers a level of precision that is essential for effective cancer treatment. A comparative study highlighted the effectiveness of 4DCBCT over 3DCBCT in image-guided radiotherapy for patients with Stage IA non-small-cell lung cancer (NSCLC). The study concluded that for small pulmonary tumors, which are particularly challenging to track due to their size and movement, 4DCBCT provides superior image guidance⁽⁴⁸⁾. This preference is based on the technology's ability to offer a more detailed and accurate visualization of the tumor, leading to better treatment precision and potentially improved patient outcomes.

However, 4DCBCT has been shown to be effective only in tracking periodic motions such as breathing and cardiac motion⁽⁴⁷⁾. Adapting the technology to monitor non-periodic

organ motion, such as movement caused by peristalsis, heartbeat, and patient movement, was necessary⁽⁵³⁾. As the movement is not regular or predictable, capturing and monitoring accurately is challenging. This unpredictability can lead to treatment inaccuracies, as the radiation may not precisely target the tumor, potentially damaging healthy tissues. To address these challenges, researchers have sought to extend the capabilities of 4DCBCT to monitor and manage non-periodic organ motion⁽⁵³⁾. This involves developing new reconstruction algorithms and techniques to capture this unpredictable movement accurately^(45,53).

Irregular breathing patterns can greatly impact the quality of images gathered through 4DCBCT and 3DCBCT⁽⁴⁷⁾. Noise degradation and streaking artifacts are the main culprits in 4DCBCT. Due to the smaller number of projections used to reconstruct each phase of 4DCBCT, image quality is typically poorer than that of 3DCBCT, which can result in streaking artifacts during each breathing phase⁽⁵⁴⁾. The amplitude of the noise power spectrum (NPS) is two times higher for the 4DCBCT than for the 3DCBCT, which could influence the visibility of fine details in the images⁽⁴⁷⁾. Despite the benefits of improved image quality and reduced motion artifacts offered by 4DCBCT, it is important to consider the higher noise levels and potential for streaking artifacts.

It is also known that the speed of the gantry rotation significantly impacts image quality and dose. Compared to 3DCBCT, the 4DCBCT image acquisition process takes longer, which can increase the risk of patient motion between imaging and treatment and give a higher radiation dose to the patient⁽³³⁾. 4DCBCT with 2 minutes per rotation provides clinical benefits by reducing intrafractional motion risk and halving patient dose⁽⁵⁴⁾, while 4DCBCT with 4 minutes per rotation offers better image quality by reducing artifacts⁽⁴⁶⁾. There is currently no standardized application scheme recommended for 4DCBCT, making it difficult to integrate into established treatment protocols. As a result, it is important to consider the risks and benefits before using this technology. The high computational demands and complexity of respiration-correlated imaging introduce additional uncertainties and require robust technical support⁽⁵⁵⁾. The high computational demands and complexity of respiration-correlated imaging introduce additional uncertainties and require robust technical support⁽³³⁾.

Additionally, patient, respiratory, and cardiac motion can contribute to image artifacts like blurriness and distortions. These artifacts can pose a challenge in accurately assessing

the position of a tumor, which is essential in making informed treatment decisions. They can negatively affect the accuracy of delivering radiation to the tumor, resulting in a dose deficiency or overdose in both the tumor and the surrounding healthy tissues. To minimize the impact of these potential artifacts, it is essential to use appropriate patient preparation and immobilization techniques such as breath-hold methods, forced shallow breathing, respiratory gating, and real-time tracking methods.

Breath-hold methods involve the patient taking a deep breath and holding it as the imaging takes place. On the other hand, forced shallow breathing methods require the patient to breathe in shallowly and hold their breath, which is useful for patients who cannot hold their breath for long periods. Respiratory gating methods synchronize the imaging with the patient's breathing cycle, while real-time tracking methods use sensors to monitor the patient's movements and adjust the imaging accordingly.

2.4. Volumetric Modulated Arc Therapy (VMAT)

In radiotherapy, conformal treatment planning techniques that cover the target volume more accurately have been developed with the increase in the use of computed tomography, which provides 3D imaging. In these treatment techniques, wedge filters are used to reduce contour irregularities and create a homogenous mixed dose distribution to protect critical organs. Though these modulators can adjust density, they are insufficient in the concave regions. Moreover, this deficiency was eliminated with the invention of the MLC, which consists of many fibres that can move independently and automatically to create a regular or irregular field. Eventually, the concept of IMRT was created. IMRT is an improved form of conformal radiotherapy. It provides a high dose to the target volume with irregular density beams or continuous arcs while protecting critical organs.

In 2007, Volumetric Modulated Arc Therapy (VMAT) was invented by utilizing the basic principles of IMRT. Cone beams of variable shape and density in the linear accelerator are rotated 360° and volumetrically apply the radiation dose to the target⁽⁵⁶⁾. Treatment may involve one or more arches. Still, at the same time, it can also be stopped and started at certain angles. This dynamic treatment delivery allows for better conformity to the tumor, reducing the risk of damaging nearby organs and tissues. In the VMAT technique, the gantry rotation speed, dose rate, and MLC shape change at the same time, and the continuous rotation of the gantry around the patient with single or multiple arc angles and simultaneous modulation of

the beam parameters make the treatment more efficient. Additionally, VMAT can be used to treat multiple tumors in a single session, further enhancing treatment efficiency.

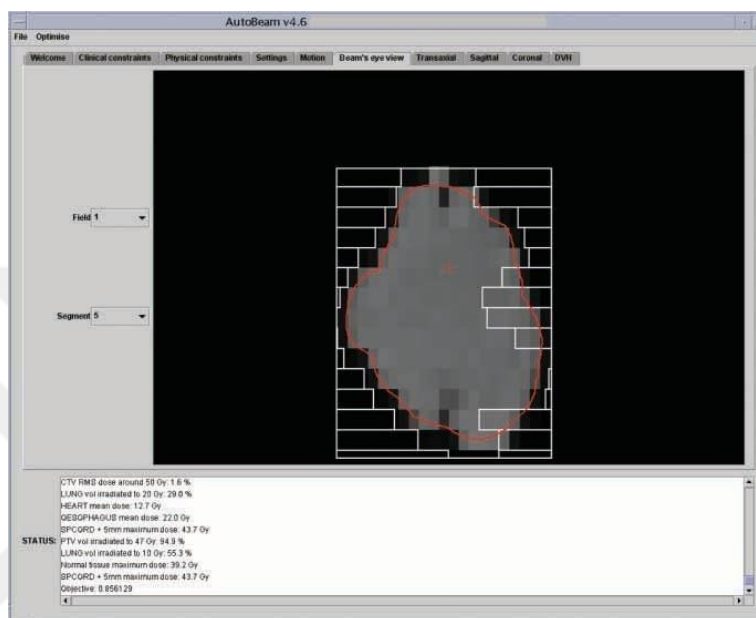


Figure 2.18. A control point in the planning system, with a fluence map in greyscale and precisely segmented MLC leaves ⁽⁵⁷⁾

The precision and accuracy of VMAT make it an ideal treatment option for complex tumors that are challenging to target with conventional radiation therapy techniques. The arc-based delivery allows for precise shaping of the radiation beam, enabling clinicians to treat irregularly shaped tumors comfortably. The increased quantity of fields and monitor units (MU) exposes a greater volume of healthy tissue to low-dose radiation ⁽⁵⁶⁾. Thus, the risk of secondary malignancy is reduced. Additionally, VMAT is a faster treatment option than fixed gantry IMRT, resulting in shorter treatment times and improved patient outcomes ⁽⁵⁸⁾.

When it comes to SBRT involving a mobile tumor, such as one in the lung, the VMAT technique is preferred. This is because it ensures that the radiation dosage is delivered to the target with exceptional precision, thereby minimizing treatment time and protecting at-risk organs. Moreover, in VMAT-SBRT plans, 1-7 coplanar or non-planar arcs are used.

VMAT for lung SBRT generates a dose distribution characterized by steep dose gradients, effectively sparing the adjacent normal tissue surrounding the tumor. However, during the actual therapy, changes in the patient's anatomy may affect the accuracy of the dose distribution ⁽⁴⁶⁾. The uncertainties resulting from patient placement and anatomical changes are commonly called the "margin" concerning the target and the organs at risk (OARs). Ensuring the accurate positioning of the tumor within the targeted radiation area while minimizing damage to other organs at risk (OARs) is a crucial aspect of high-precision radiation therapy.

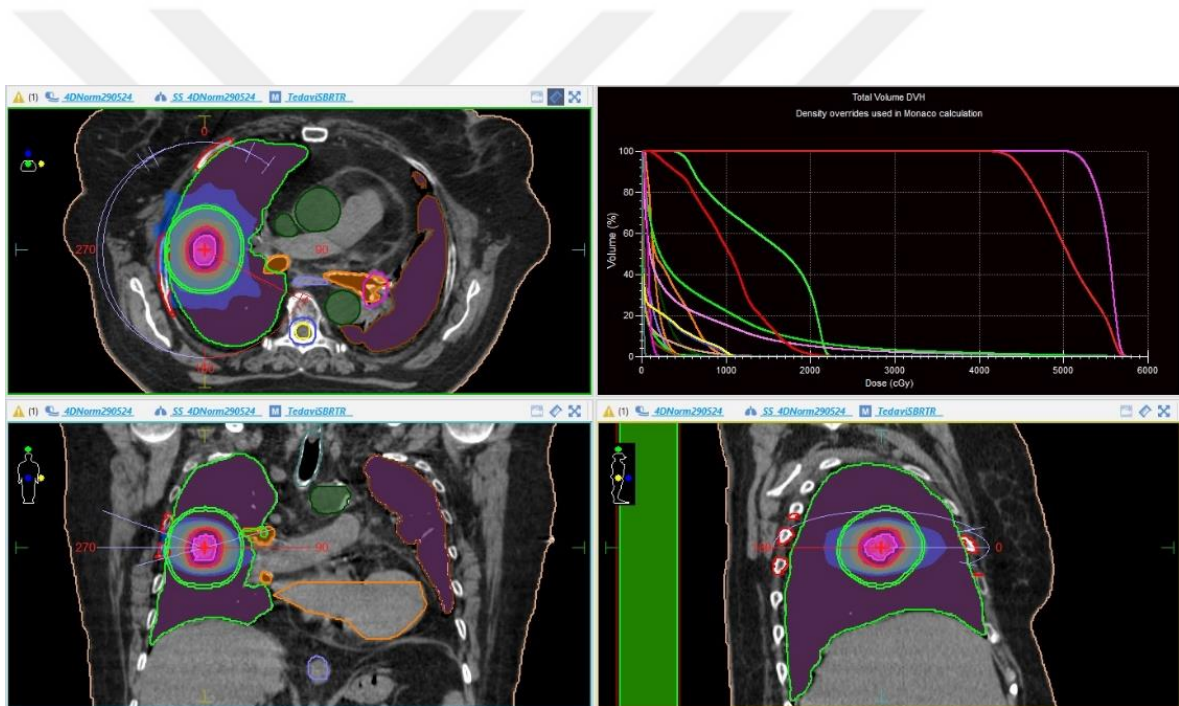


Figure 2.19. Axial, sagittal, and coronal images for a VMAT plan. The pink-shaded structure represents ITV, and the green-shaded area represents PTV.

3.

MATERIAL AND METHODS

3.1. Patient Selection

Our study involved a retrospective analysis of 19 patients between 2018-2023 diagnosed with either early-stage non-small cell lung cancer or single-lesion metastatic cancer. We utilized the TNM staging system to categorize each patient, where T1-2 indicates the size and extent of the primary tumor, N0 signifies no regional lymph node involvement, and M0 denotes the absence of distant metastasis. A significant proportion of the patients (11 out of 19) were diagnosed with metastasis. Six out of 19 patients were diagnosed with early-stage NSCLC (T2N0), and one patient was diagnosed with early-stage NSCLC (T1N0M0).

Among these patients, four had two distinct lesions in different areas, totaling 23 tumors assessed across various sites. The anatomical distribution of these lesions was as follows: 12 were classified as peripheral lesions, 2 were located in proximity to the diaphragm, 1 was centrally located near the heart, and the remaining were categorized as 4 central and 4 chest wall lesions. Specifically, in the left lung, we observed 7 lesions in the left upper lobe (LUL), 3 in the left lower lobe (LLL), and 2 in the left middle lobe (LML). In contrast, the right lung exhibited 5 lesions in the right upper lobe (RUL), 3 in the right lower lobe (RLL), and 3 in the right middle lobe (RML).

We are delighted to announce that the Non-Interventional Clinical Research Ethics Committee of T. C. Yeditepe University has approved our study under application number 202105057. This approval facilitates our ongoing research efforts and underscores the ethical standards upheld throughout our study.

Table 3.1 Characteristics of the 19 patients and diseases.

Patient	Age	Sex	TNM Stage	Patient	Age	Sex	TNM Stage
1	73	M	Metastasis	11	55	M	Metastasis
2	82	M	Metastasis	12	77	M	T2NO
3	68	M	Metastasis	13	56	M	T2NO
4	64	F	T2NO	14	66	M	Metastasis
5	36	F	Metastasis	15	75	M	T2NO
6	68	M	T1NOMO	16	69	M	Metastasis
2	82	M	Metastasis	17	36	F	Metastasis
7	75	M	Metastasis	17	36	F	Metastasis
7	75	M	Metastasis	18	82	F	Metastasis
8	58	F	Metastasis	18	82	F	Metastasis
9	67	F	T2NO	19	76	M	Metastasis
10	65	M	T2NO				

3.2. Simulation and Delineation

We performed 4DCT planning scans for each patient using a GE Discovery RT Gen 2 CT simulator to capture detailed and accurate tumor movement and morphology information. Patients were positioned supine with their arms elevated above their heads and immobilized using either a wing board or a vacuum bag. This setup was employed to minimize any movement during the scan, thereby ensuring precise documentation of tumor behavior.

For tumors located near the diaphragm, we employed a technique of abdominal compression. This involved applying external pressure below the sternum to limit diaphragmatic motion, consequently reducing tumor displacement caused by breathing and enhancing the accuracy of our results.



A

B

Figure 3.1. Immobilization of Patient using (A) a wing board, (B) a vacuum bag, and abdominal compression.

We employed the Smart Deviceless 4D feature provided by GE Medical Systems to enhance the precision of our planning 4DCT images, which incorporate the dynamics of the patient's respiratory cycle. This advanced feature employs a wire to construct a patient's respiratory pattern model. The patient's position is confirmed through a topogram image by the device to verify the accuracy. Additionally, it assesses the respiratory cycle duration using a monitor scan before the simulation process. This capability facilitates real-time observation of the patient's respiratory movements, which is crucial for accurate treatment planning. Upon acquisition, the 4DCT images are automatically categorized into respiratory phase bins in cine mode. The average of these cine CT raw images is calculated, and the images are subsequently processed and binned by the device's software to generate accurate, real images.

To generate the patient's respiratory pattern, we utilized a wire. We conducted multiple CT scans, each at a slice thickness of 1.25 mm while allowing the patients to breathe freely. The CT images derived from the sinusoidal curve produced by the wire during the respiratory cycle were integrated with images from the sinusoidal curve resulting from the table's movement. This integration process produced images depicting 10 distinct phases of the respiratory cycle, providing a more detailed and precise assessment of tumor motion and

morphology. This approach enabled a detailed and comprehensive analysis of the tumor's behaviour.



Figure 3.2. Utilizing a wire to create the respiratory pattern during the 4D-CT.

The 4DCT images produced were subsequently reconstructed to create MIP (Maximum Intensity Projection), Min IP (Minimum Intensity Projection), and AIP (Average Intensity Projection) images. These images were then imported into the Monaco 6.1.2 version treatment planning system. Our study encompassed 19 patients with lesions situated in various locations, including peripheral, central, chest wall, and diaphragm regions.

The radiation oncologist meticulously delineated all organs at risk (OAR) and target volumes, ensuring no planning bias was introduced. The same radiation oncologist manually outlined the Gross Tumor Volume (GTV) and Internal Target Volume (ITV) in the lung window to ensure uniformity across all cases.

For patients with tumors distant from critical structures such as the heart, chest wall, and diaphragm, ITVs were constructed using Maximum Intensity Projection (MIP) images. Conversely, a more detailed approach was employed for tumors proximal to the chest wall and diaphragm using images from 10 different respiratory cycle phases. This method

involved isolating the GTVs for each phase and amalgamating these GTVs to form the ITV on the planning Computed Tomography (CT) scan.

Subsequently, the generated ITVs were transposed onto the planning CT scan captured during normal breathing and all other critical organs were contoured on the norm CT. The treatment planning was then carried out using the norm CT scan.

In routine clinical practice, an isotropic 5mm margin is generally used to create the Planning Target Volume (PTV) margin. However, for our study, an isotropic margin ranging from 3 to 7 mm was applied depending on the lesion's location and volume to account for setup inaccuracies from all directions while encompassing the area targeted for radiation therapy.

The detailed table below provides the tumor volumes and locations for each patient, playing a crucial role in determining the appropriate radiation dose and target volume for each case.

Table 3.2. The tumor characteristics and margins of the 19 patients in this study.

Patient	Tumor Localization	Zone Classification	ITV (cc)	Margins(mm)	PTV (cc)
1	LML	Central	4.958	5	20.227
2	LUL	Chest-wall	0.524	6	5.8
3	LUL	Peripheral	0.715	5	5.166
4	RML	Chest-wall	22.512	4	47.281
5	LML	Central	11.081	4	23.636
6	RUL	Peripheral	7.335	4	19.283
2	RUL	Peripheral	1.357	5	7.355
7	LUL	Peripheral	0.754	5	5.169
7	RUL	Peripheral	1.376	7	11.376
8	LLL	Peripheral	0.428	5	5.583
9	RML	Central	9.321	4	27.091
10	RLL	Peripheral	11.270	5	35.383
11	RUL	Peripheral	32.569	3	60.835
12	RUL	Central	29.371	4	58.065
13	RML	Peripheral	6.949	5	28.269
14	LLL	Peripheral	3.563	6	16.387
15	LUL	Peripheral	3.99	5	14.823
16	RLL	Diaphragm	28.585	4	55.445
17	LUL	Peripheral	0.25	5	3.3
17	LUL	Central close to heart	0.947	5	6.250
18	RLL	Chest-Wall	3.219	5	14.244
18	LLL	Diaphragm	4.548	4	15.064
19	LUL	Chest-Wall	1.203	5	7.676

*ABBREVIATIONS: LLL = left lower lobe; LML = left middle lobe; LML = left middle lobe, LUL = left upper lobe; RLL = right lower lobe; RML = right middle lobe; RUL = right upper lobe.

3.3. Treatment Planning

Following the margin determination, we advanced to the treatment planning stage. We formulated Volumetric Modulated Arc Therapy (VMAT) treatment plans utilizing either four or five arcs, employing 6 MV flattening filter-free (FFF) photon beams. The primary goal was to achieve sharp dose gradients, precise localizations, and elevated doses per fraction in extracranial sites, adhering to RTOG clinical protocols. We meticulously set the appropriate optimization parameters, such as organs at risk (OARs), dose constraints, and specific tumor doses, to meet this goal.

We utilized the Monte Carlo algorithm to calculate dose distribution, marking the initial use of this algorithm in the Monaco treatment planning system to meet the required dose intensity map specifications. Following the initial optimization, we optimized the segment shape within the Monaco system to configure the segments for arc. We thoroughly evaluated the Dose-Volume Histograms (DVH) resulting from this segment shape optimization. Upon completing the segmentation process, normalization was done to ensure that the clinical doses for organs at risk (OARs) aligned with the DVH assessments. Below are examples of patient treatment plans and the approved DVH (Dose-Volume Histogram) values for reference.

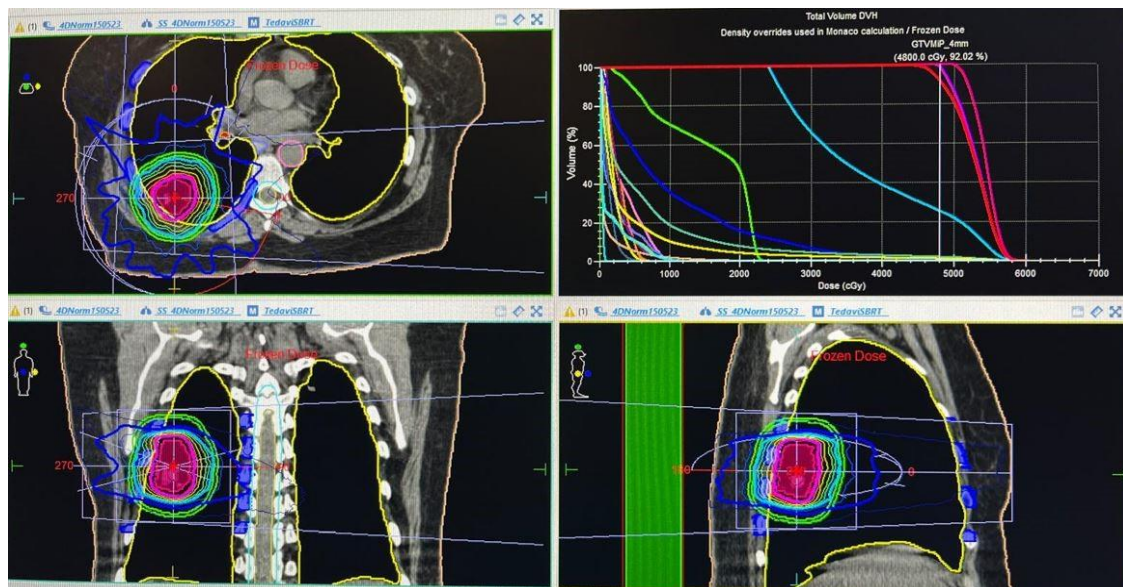


Figure 3.3. Treatment plan and the corresponding DVH values.

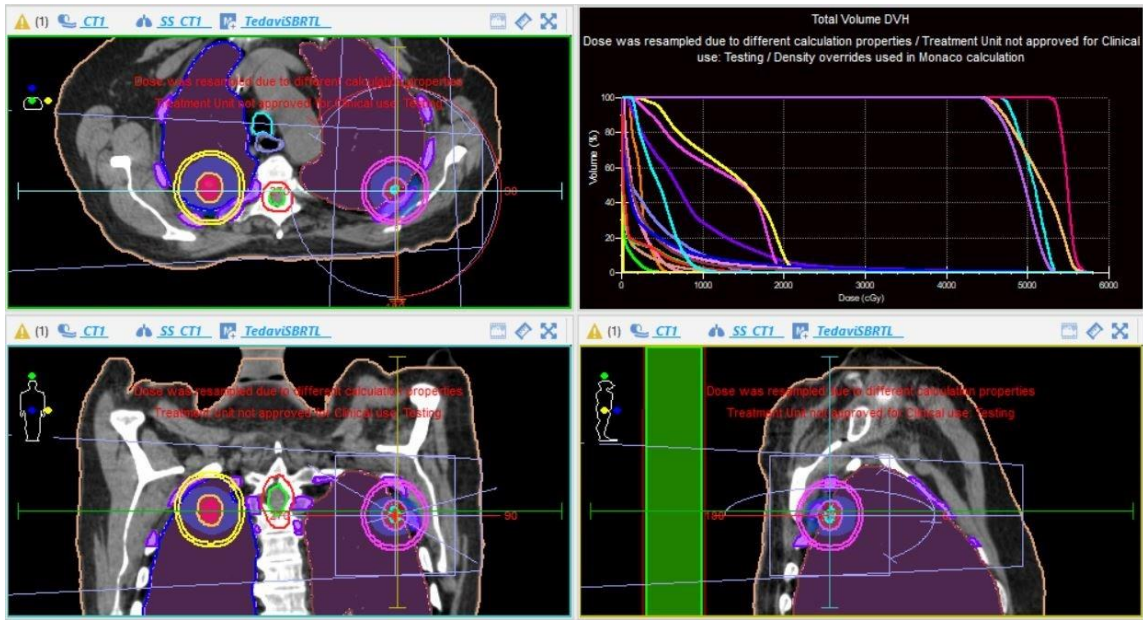


Figure 3.4. Treatment plan of two different lesions and their corresponding DVH values.

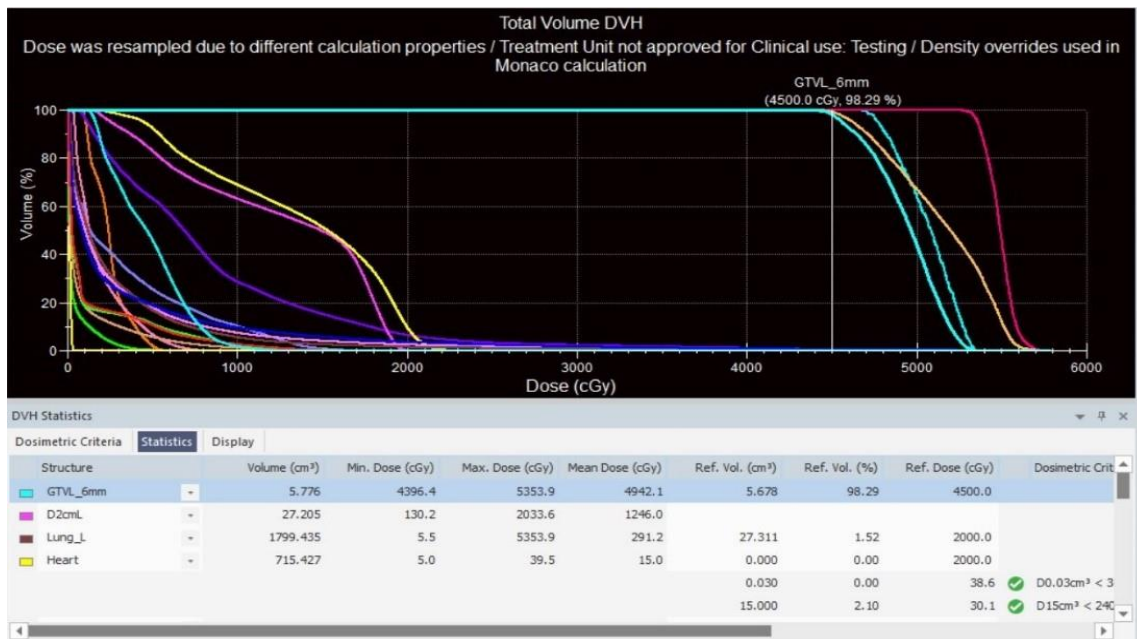


Figure 3.5. DVH Statistics

Fractionation and dose schedules were determined according to RTOG protocols, with treatment planning acceptance criteria based on the dose constraints established by these guidelines. In our research, patients received radiation therapy with doses ranging from 24 to 60 Gy, administered in 1 to 8 fractions depending on the zone and lesion location. Our results indicated that the maximum dose coverage for the Planning Target Volume (PTV) varied from a minimum of 70% to a maximum of 98.29% of the prescribed dose. Below is a detailed table summarizing our patients' dose and fractionation schedules, along with their respective percentage coverage values, providing a comprehensive overview of the treatment outcomes.

Table 3.3. Patient Dose, Fractionation Schedule, and Respective percentage coverage values.

Patient	Dose/Fraction	Coverage%	Patient	Dose/Fraction	Coverage%
1	60Gy/8 fx	70	11	60Gy/3 fx	72.57
2	45Gy/3 fx	92	12	60Gy/3 fx	92
3	50Gy/5 fx	83	13	54Gy/3 fx	82
4	45Gy/3 fx	94.38	14	54Gy/3 fx	90.99
4	45Gy/3 fx	98.29	15	45Gy/5 fx	91
5	24Gy/1 fx	90.93	16	45Gy/3 fx	90.52
5	24Gy/1 fx	92.02	16	45Gy/3 fx	84.33
6	30Gy/1 fx	95.37	17	45Gy/4 fx	84.42
7	45Gy/3 fx	85.68	17	45Gy/3 fx	90.96
8	50Gy/5 fx	83	18	45Gy/3 fx	95.02
9	50Gy/5 fx	90	19	48Gy/4 fx	92.02
10	45Gy/5 fx	91			

After the SBRT plans were completed, treatment quality assurance (QA) was performed for each patient prior to treatment to assess deliverability.

3.4. Treatment

3.4.1. Treatment Machine: Elekta Versa HD

Our study utilized the Versa HD (Elekta) linear accelerator at Istanbul Oncology Hospital, demonstrating effective results for Stereotactic Body Radiation Therapy (SBRT). This device incorporates a treatment head and supports the Volumetric Modulated Arc Therapy (VMAT) technique, facilitating reduced treatment durations for SBRT.

The Versa HD Elekta is equipped with advanced technology that allows clinicians to visualize and treat tumors with exceptional precision. It features 4D imaging technology and an advanced treatment delivery system that accurately tracks tumor movement. A significant technological enhancement of the Versa HD Elekta is its capability for mean-time tracking, allowing for monitoring average times associated with various processes such as setup, beam delivery, and overall treatment.

A distinctive attribute of the Versa HD Elekta is its sophisticated 'Agility' multi-leaf collimator (MLC), which includes a 160-leaf system. This system achieves remarkable precision in radiation shaping, with each leaf featuring an isocenter width of 0.5 cm, a maximum velocity of 6.5 cm/s, and an optical system-based leaf transmission under 0.5%. The MLC's design permits precise radiation delivery to the tumor while protecting adjacent healthy tissues, effectively minimizing exposure to non-target areas.

Furthermore, the device's High Dose Rate mode, known as Flattening Filter Free (FFF), enhances the speed of treatment delivery, thereby shortening patient time in the treatment room and improving machine throughput.

The Versa HD Elekta also incorporates the HexaPOD™ evo RT system, a leading-edge stereotactic treatment enhancement. This system directly integrates robotic couchtops with six degrees of freedom into the standard table, ensuring supreme precision in radiation delivery. The HexaPOD™ evo RT gives clinicians the confidence to handle complex cases with unparalleled accuracy, ensuring meticulous execution of each treatment session.



Figure 3.6. Istanbul Oncology Hospital LINAC device: Elekta Versa HD

3.4.2. Treatment Procedure

Before proceeding with the treatment, we ensured the patient was thoroughly informed about the process. We provided detailed explanations of each step and addressed any queries or concerns they might have had. Once the patient consented and was prepared, we arranged the immobilization device, previously used during the 4DCT, for the treatment session.

We accurately positioned the patient using CT scans and adjusted the shifting values according to the treatment plans for precision and accuracy. Additionally, kV-kV images were taken during the setup stage to replicate the patient's positioning with millimetric precision.

3.4.2.1. 4DCBCT pre-treatment and Symmetry software

4DCBCT scans are performed in the treatment room to acquire detailed images of the tumor and surrounding anatomy. The patient is positioned in the same manner as for the treatment.

In order to ensure precise alignment of the target, we utilized the Elekta XVI (X Ray Volume Imaging, Elekta, Stockholm, Sweden) device to capture 4DCBCT images. The scan parameters were specifically set to Chest M20 F1 to obtain the necessary data for accurate target alignment. We then utilized the Symmetry software to combine these images, creating a comprehensive representation of the target area.

The 4DCBCT system on the Elekta Versa HD uses the Symmetry XVI software to capture respiratory movements and manage variations across different treatment sessions. Instead of generating a MIP image from multiple scans, this system visualizes tumor displacement around its central point, highlighting the location where the tumor is most frequently positioned, known as the mean time-weighted target position. This important information helps optimize radiation therapy planning, enabling physicians to optimize the radiation dose and target the most effective delivery site.

One of the useful tools in symmetry software is the Clipbox feature. The Clipbox feature is essential for isolating specific areas within an image, enhancing visibility and attention to targeted regions, such as tumors or other focal points. This is crucial for evaluating the accuracy of patient setup.

Another handy tool in symmetry software is the Mask feature. The mask feature in Symmetry software significantly emphasizes particular areas or features within an image. It is used to "mask" certain aspects, aiding in identifying and accentuating critical areas like tumors and facilitating treatment planning.

During the planning phase, we used the Symmetry system's Dual Matching feature to map 4DCT to 4DCBCT. We employed the rectangular Clipbox option in the 4D image to match the stationary image of the tumor, unaffected by movement. Next, we performed mask matching, where we created a virtual mask structure to select the region where the tumor moves during the breathing cycle. Then, we added a 5 mm margin to the generated GTV (Gross Tumor Volume) to create a virtual lesion. To ensure accurate definition of the region of interest, we manually removed all bone structures, such as ribs, vertebrae, and sternum, using a drawing tool.



Figure 3.7. 4DCBCT Symmetry Protocol Clip box Matching: Bone Structure

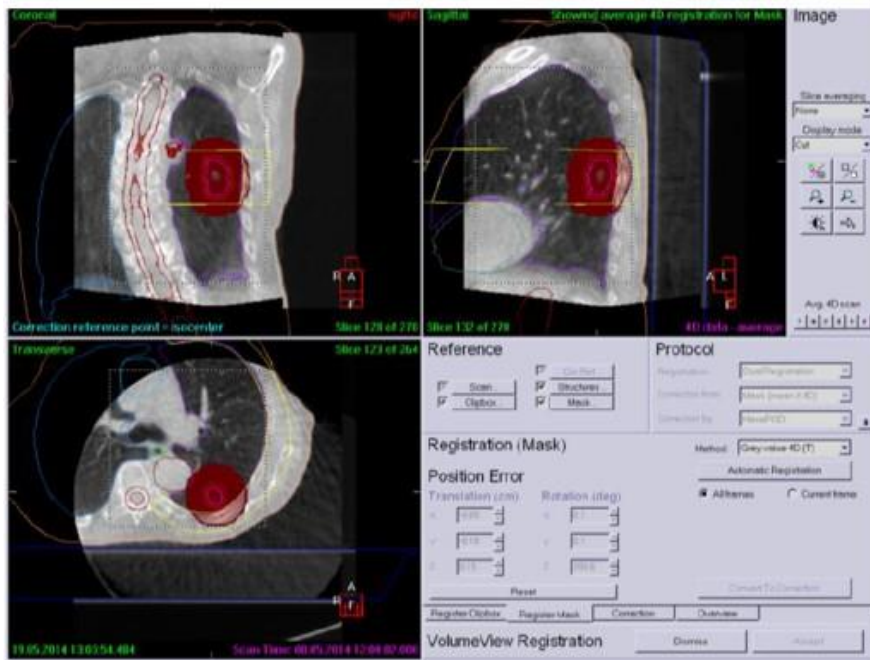


Figure 3.8 Mask Matching: Mapping GTV for each phase of respiration.

As a result, if there is a baseline shift error due to the patient's position, we corrected it with the clipbox registration. For movement-related errors, we corrected them with the mask registration.

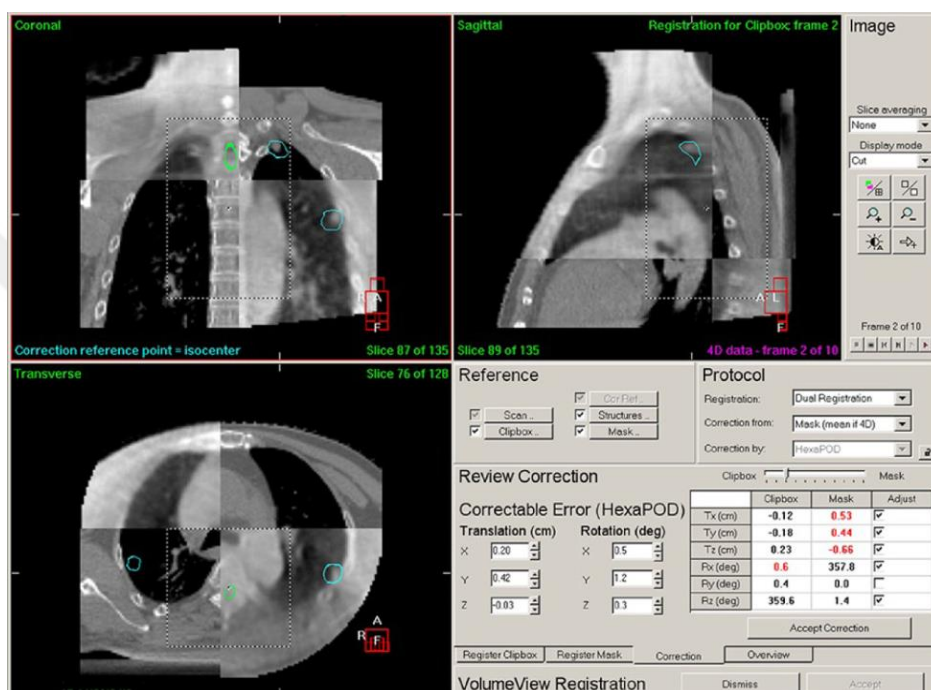


Figure 3.9. Correlation of position errors obtained from Clipbox and Mask registration

Treatment commenced only when all setup errors were confirmed to be within 1 or 2 mm, guaranteeing that the treatment was conducted with utmost precision and safety. If setup errors exceeded 2 mm, adjustments were made by shifting the treatment couch and acquiring a second CBCT. This process was repeated until the residual error was reduced to less than 2 mm. By meticulously measuring and minimizing residual errors, we ensured that the treatment administered to the patient was highly accurate and effective.

SBRT treatment was then applied with online correction using pre-treatment 4D CBCT with 10-phase images. Adhering to the manufacturer's standard image acquisition and reconstruction settings, we conducted a 200° rotation, capturing 1320 frames over 4 minutes,

using settings of 20 mA, 16 ms per frame, 120 kV, and an S20 filter. This protocol allowed us to capture high-quality images while minimizing radiation exposure, and we successfully obtained a respiration-correlated 4DCBCT during the treatment delivery.

While the treatment duration varied depending on the number of arcs, it typically ranged between 15 to 25 minutes.

3.5. Image Transfer and Registration Method

In our study, we analyzed a total of 80 sets of 4DCBCT images, dependent on the number of treatment fractions and lesions per patient. We utilized 4DCBCT images processed through Symmetry XVI software, which were individually transferred to each patient's Monaco treatment planning system using back projection.

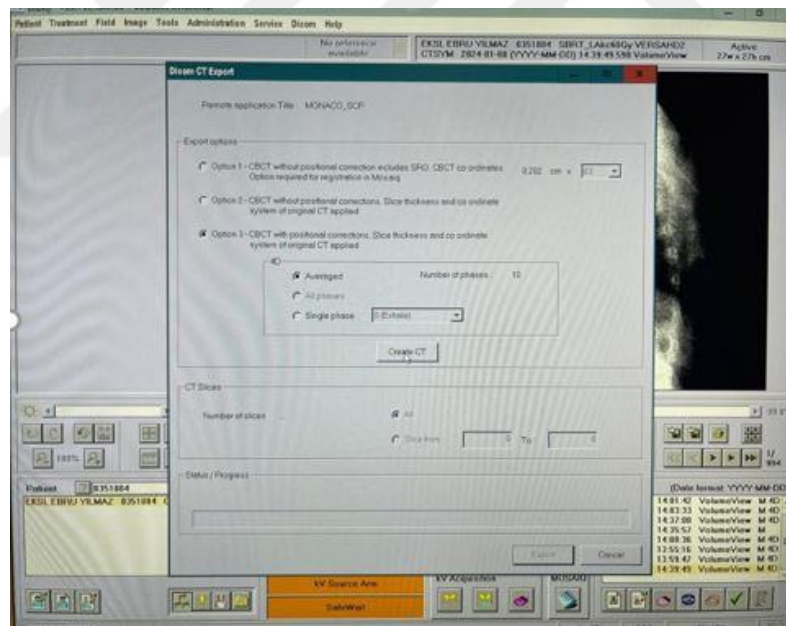


Figure 3.10. Transmission of 4DCBCT images to the Monaco treatment planning system using back projection.

These 4DCBCT images were then fused with 4DCT images acquired during the simulation phase.

3.5.1. 4DCT and 4DCBCT Image Registration

Rigid image registration aims to align images obtained from different time points or different imaging devices, ensuring that the anatomical structures in the region of interest are accurately matched for comparison and analysis. Rigid image registration involves translation, rotation, and scaling of the images but does not account for complex tissue deformations.

We aligned the Maximum Intensity Projection (MIP) or 10 phase images with the 4D CBCT images using a rigid image registration method. After the alignment, we carefully checked the accuracy of the registration process and made any necessary adjustments to ensure precision. This usually involved a thorough visual inspection and, when possible, quantitative measures to confirm the alignment. By combining these images, we were able to accurately assess tumor displacement in the right-left (RL), superior-inferior (SI), and anterior-posterior (AP) directions. We achieved this by comparing the planned Internal Target Volume (ITV) from the 4DCT images with the actual tumor positions observed in the 4DCBCT images taken during pre-treatment.

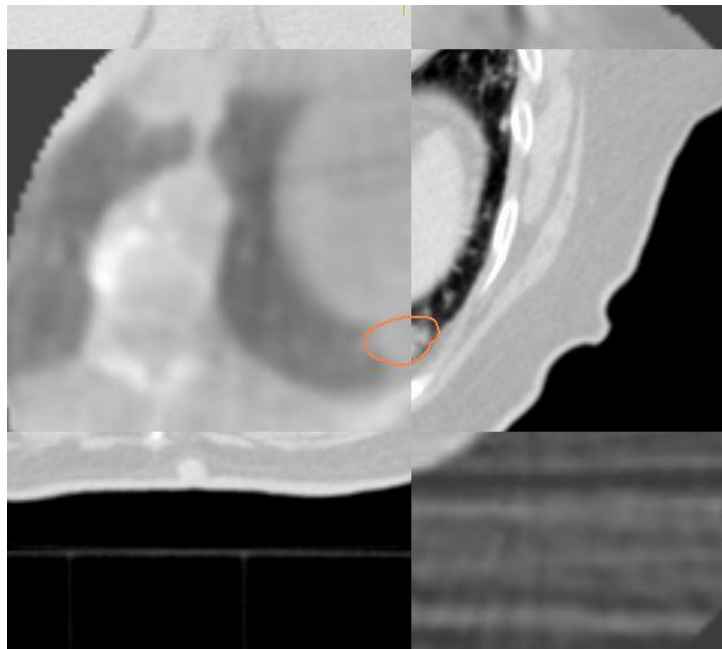


Figure 3.11. Matching 4DCT and 4DCBCT images for a single fraction with a diaphragm lesion in a patient

3.5.2. Delineation of 4DCBCT to Define GTV Volume

The primary objective of delineating the Gross Tumor Volume (GTV) on 4DCBCT is to accurately locate the tumor on the images taken before or during the radiation treatment session. 4DCBCT is utilized for this purpose due to its mean time-weighted imaging capabilities, which allow for the visualization of any changes in the tumor's size, shape, or position caused by patient movement, physiological processes, or treatment response.

The Internal Target Volume (ITV) was delineated from the 4D CT images and for each fraction the Gross Tumor Volume (GTV_{4DCBCT}) on 4DCBCT was consistently delineated by the same radiation oncologist. To ensure the stability of the tumor location, GTVs in each fraction of 4DCBCT images were determined using lung window settings for each patient to ensure consistency in target volume delineation. This process involved outlining the tumor contours on each slice of the CBCT scan where the tumor is visible. This approach is crucial for evaluating setup errors and assessing the impact of respiratory motion on tumor localization.

In conclusion, at Part I of our study, we determined the tumor volume, its motion, and the central position of the tumor using both planning 4DCT and 4DCBCT, which were obtained prior to each SBRT fraction. Part II involved assessing the tumor motion and evaluating the PTV margin utilized in the 4D CT. We compared the centroid position of the tumor along the three axes in the mean-time 4DCBCT with the 4DCT to determine the vectoral displacement of the tumor center. In Part III, we used SPSS software (version to 25.0 be specified) to calculate the mean offset values, standard deviation of the vectoral displacement, and conducted a t-test to statistically analyze the Pearson correlation between both data sets concerning tumor volume, location, and patient age.

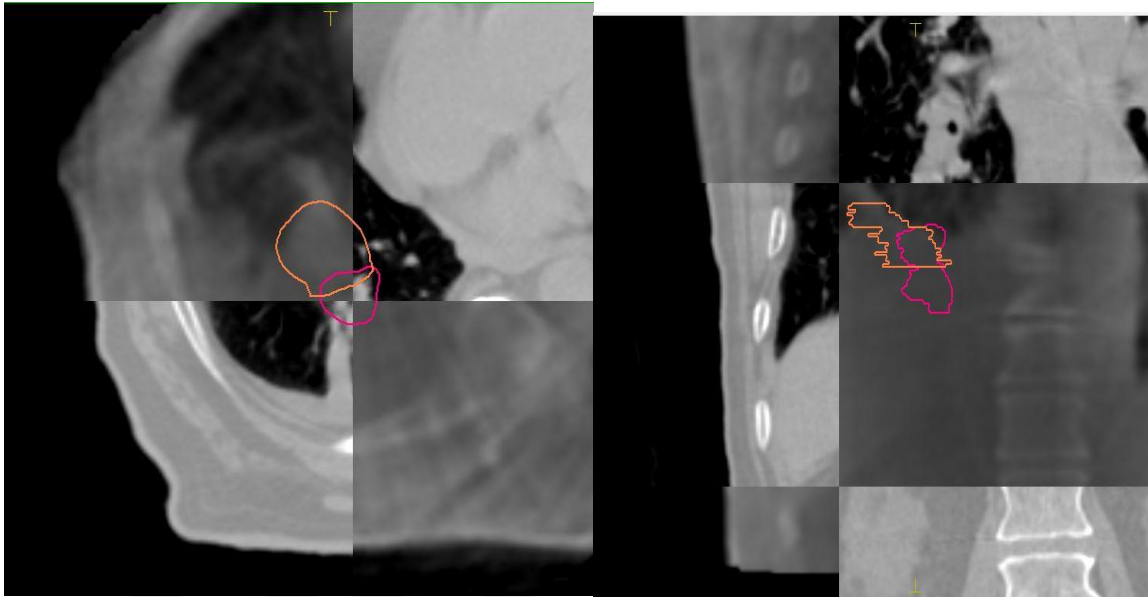


Figure 3.12. Delineation of GTV for a single fraction of 4DCBCT and ITV in 4DCT images, with using lung window level in a diaphragm lesion

3.5.3. Comparison of the centroid positions of ITV and GTV_{4DCBCT}

The centroid position in 4DCT and 4DCBCT refers to the geometric center of the tumor, determined by the position of all tumor voxels in three-dimensional space.

In 4DCT, this position is established during the planning phase, capturing the tumor's movement across different phases of the breathing cycle, which aids in accurate tumor delineation and treatment margin planning.

In contrast, in 4DCBCT, the centroid position is assessed before each SBRT fraction. This modality not only captures the tumor's movement but also allows for mean-time verification and adjustments, ensuring precise targeting of the radiation treatment despite respiratory motion.

By comparing the centroid positions obtained from 4DCT and 4DCBCT, we can evaluate the consistency of tumor motion and the accuracy of the planned treatment margins.

To accurately calculate the centroid position for each segmented volume, we identified specific interest points on both the Internal Target Volume (ITV) and the GTV_{4DCBCT} . This involved marking specific points within these volumes and extracting the coordinates (x, y, z) of all points within the segmented region to represent the voxel locations

within the 3D volume. Subsequently, we determined the centroid coordinates by averaging the positions of all points in the segmented region, providing a more accurate representation of the central position of the volumes.

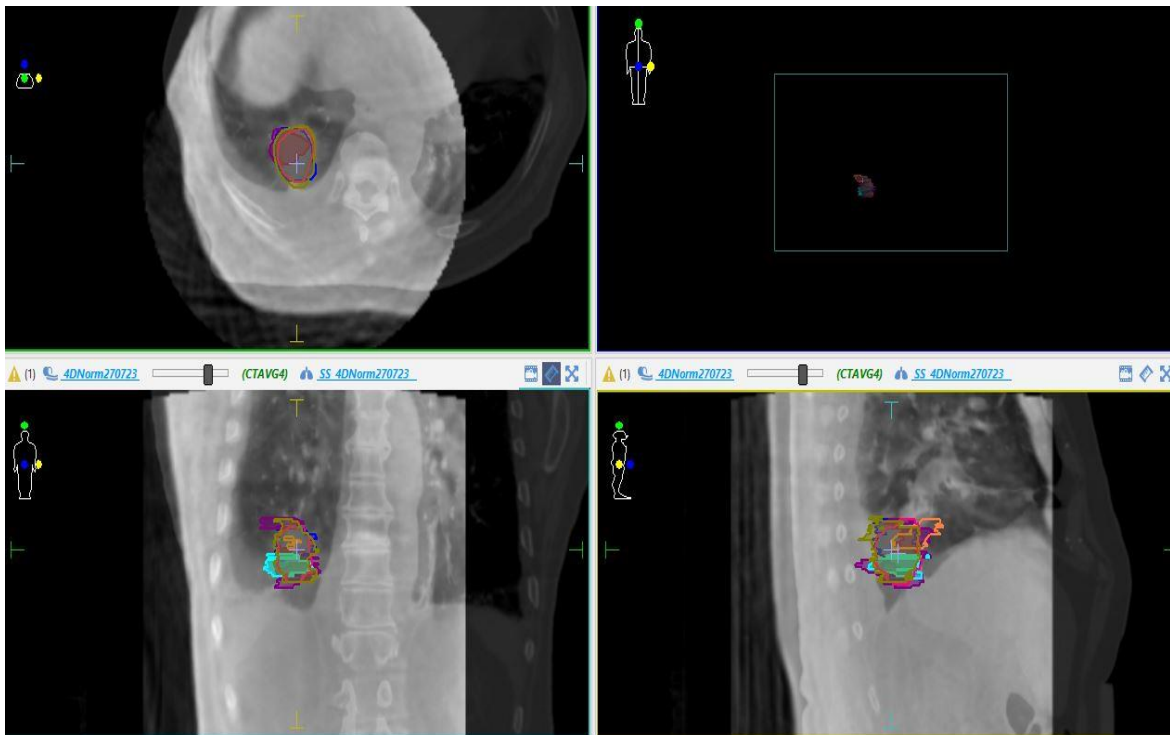


Figure 3.13. Place interest points for calculating the centroid positions in the 4DCBCT and ITV fusion images for a diaphragm lesion.

Following this, we calculated the vectorial difference between the centroid position of the ITV transposed onto the 4D Cone Beam Computed Tomography (CBCT) images and the centroid position of the Gross Tumor Volume (GTV_{4DCBCT}) during CBCT. This calculation involved measuring the displacement between the central point of the ITV as planned from earlier imaging phases and the actual central point of the tumor volume as captured in the 4D CBCT scan. This detailed approach allowed us to precisely assess the differences in position

between the planned and actual central points of the volumes, providing valuable insights for further analysis.

The combined images were used to evaluate the adequacy of the Planning Target Volume (PTV) margins for each tumor, allowing for a detailed examination of each patient's specific circumstances and the sufficiency of the PTV margins. All centroid positions are defined in the x, y, z direction which demonstrates the direction of the right-left (RL), superior-inferior (SI), and anterior-posterior (AP) directions of the patients.

The variation (V) between the centroid positions is defined as a motion amplitude vector variation. This variation is quantified by calculating the vector length for each patient using the following formula:

$$V = \sqrt{RL^2 + SI^2 + AP^2} \quad (1)$$

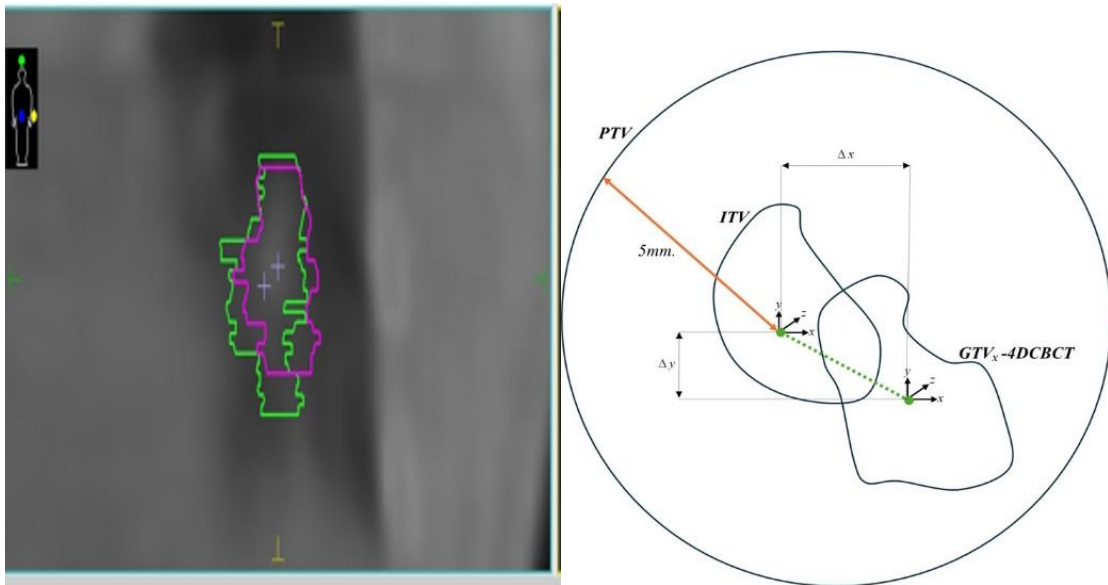


Figure 3.14. The variation between centroid positions of ITV and GTV_{4DCBCT} in (x-y) coordinates

4. RESULT

4.1. General Analysis

This study explores the important aspect of Gross Tumor Volume (GTV) localization in patients undergoing Lung SBRT, particularly focusing on how the position of the tumor varies. We collected data from planning 4D CT scans and multiple treatment fractions verified with 4D-Cone Beam CT (CBCT) scans. This data provides detailed insights into the GTV centroid positions in the right-left (RL), superior-inferior (SI), and anterior-posterior (AP) directions for each treatment fraction.

Our study included 23 cases with lung tumors, ranging from early-stage lung cancer to metastases with one or more lesions, all treated with thoracic SBRT at Istanbul Oncology Hospital. The localization of all tumors was determined using 4DCT, and image-guided radiotherapy was performed with 4DCBCT guidance before each treatment session. For each patient, we collected between 1 and 8 4DCBCT scans, depending on the number of treatment fractions.

We meticulously calculated the centroid position differences between the 4DCT and 4DCBCT scans for each treatment fraction, measuring in millimeters. This precision allows us to highlight the variability in tumor position due to physiological changes and setup errors. For example, in one patient with a left middle lesion, the maximum differences observed were 3.80 mm in the RL direction, 3.40 mm in the SI direction, and 1.30 mm in the AP direction across five treatment fractions. These measurements provide a clear picture of how much the tumor position can vary.

The dataset includes measurements from all 23 cases, with centroid positions recorded in centimeters, as used in the Monaco Treatment Planning System (TPS). We calculated the variation in the centroid position of each tumor from the 4DCT and 4DCBCT scans in millimeters to compare with the 5 mm PTV margin. This comparison highlights the differences and ensures precise targeting for effective treatment.

Table 4.1. The Variation between GTV and ITV Centroid Position.

Lesion number	GTV Localization	GTV Volume (cc)	ITV Centroid Position (cm)			#fx	GTVx-4DCBCT Centroid Position (cm)		
			RL	SI	AP		RL	SI	AP
1	LML	4.757	-2.28	9.55	-3.40	1	-2.53	9.21	-3.41
		4.729				2	-2.65	9.52	-3.47
		3.827				3	-2.53	9.43	-3.51
		3.988				4	-2.40	9.37	-3.52
		2.657				5	-1.90	9.51	-3.27
2	LUL	0.658	5.00	9.85	-9.83	1	5.25	9.88	-9.59
		0.697				2	5.00	9.76	-9.83
		0.749				3	5.13	9.98	-9.60
		0.634				3	5.50	9.85	-9.38
3	LUL	0.549	8.03	8.25	-5.87	1	7.90	8.22	-5.94
4	RML	10.069	-8.28	-8.71	-8.08	1	-8.77	-8.77	-8.20
		9.911				2	-8.53	-8.78	-8.25
		10.814				3	-8.53	-8.74	-8.22
		13.516				4	-8.28	-8.74	-8.25
5	LML	14.042	3.05	3.05	-8	1	3.31	3.35	-8.21
		12.885				2	3.16	3.48	-8.03
		11.04				3	3.29	3.35	-8.25
		12.982				4	3.29	3.48	-7.92
		11.118				5	3.39	3.35	-8.33
		14.082				6	3.26	3.48	-7.9
		11.219				7	3.3	3.35	-8.08
		10.896				8	3.03	3.23	-8.05
		6				RUL	4.463	-7.01	9.43
3.976	2		-6.8	9.18	-5.82				
4.578	3		-6.88	9.3	-5.57				
7	RUL	0.845	-5.61	5.5	-9.57	1	-5.59	5.63	-9.25
		0.956				2	-5.69	5.38	-9.02
		1.008				3	-5.6	5.63	-9.1
8	LUL	0.541	7.03	10.38	-7.5	1	7.04	10.38	-7.3
9	RUL	0.754	-5.38	4	-10.46	1	-5.2	4.13	-10.1
10	LLL	0.298	3.68	7.55	-10.39	1	3.6	7.55	-10.5
		0.326				2	3.6	7.55	-10.44
		0.62				3	3.66	7.43	-10
11	RML	11.497	-4.28	5.35	-8.23	1	-4.34	5.35	-8.5
		11.148				2	-4.05	5.35	-8.78
		14.68				3	-4.39	5.23	-8.59
		12.706				4	-4.41	5.23	-8.67

		12.956				5	-4.39	5.35	-8.77
12	RLL	15.783	-7.14	-2.63	-9.55	1	-7.56	-2.88	-9.2
		14.376				2	-7.21	-2.75	-9.41
		14.068				3	-7.14	-3.13	-9.34
		13.488				4	-7.36	-3.38	-9.42
		14.315				5	-7.06	-2.75	-9.46
13	RUL	34.568	-8.59	9.5	-4.53	1	-8.19	9.38	-4.63
		40.382				2	-8.37	9.63	-4.59
		38.955				3	-8.2	9.88	-4.6
		37.556				4	-8.4	9.75	-4.6
		37.05				5	-8.53	10	-4.61
14	RUL	21.02	-4.42	1.88	-8.83	1	-4.49	2.13	-9.06
		20.835				2	-4.39	2.13	-8.77
		23.178				3	-4.4	2.25	-8.8
15	RML	5.431	-8.95	5.9	-1.8	1	-9.09	6.03	-1.59
		4.636				2	-9.22	6.15	-1.68
		4.892				3	-9	6.03	-1.6
16	LLL	4.578	6.63	-6.13	-9.47	1	6.89	-6	-9.27
		3.431				2	6.7	-6	-9.4
		5.894				3	6.8	-6	-9.4
17	LUL	4.569	7.36	2.5	-6.18	1	7.4	2.75	-5.8
		3.672				2	7.5	2.75	-5.82
		4.695				3	7.68	3	-5.57
18	RLL	16.004	-6.61	-6.55	-5.97	1	-7.33	-7.43	-5.55
		28.048				2	-7	-6.55	-6.3
		24.843				3	-6.7	-6.43	-6.3
		35.526				4	-6.57	-6.3	-6.54
19	LUL	0.268	4.7	4.35	-3.5	1	4.74	4.35	-3.43
		0.238				2	4.8	4.35	-3.4
		0.297				3	4.8	4.23	-3.5
20	LUL	0.521	6	1.25	3.9	1	5.91	1.25	3.89
		0.537				2	6.1	1.25	3.9
		0.418				3	5.9	1.25	4
21	RLL	3.796	-5.7	3.45	-7.2	1	-5	3.95	-7.2
		2.845				2	-5.2	3.83	-6.8
		3.441				3	-5.3	3.7	-6.9
		2.931				4	-5.3	3.83	-6.9
22	LLL	6.227	6.08	-8.4	-10.7	1	5.93	-7.9	-10.66
		6.31				2	6	-8.03	-10.8
		6.291				3	5.9	-7.78	-10.5
23	LUL	1.45	6.49	7.3	-6.37	1	6.4	6.9	-6.3
		2.1				2	6.5	7.15	-6.5
		1.929				3	6.4	6.9	-6.3

4.1.1 Intra Fraction Motion Evaluation

The mean, median, and standard deviation of the centroid positional differences were meticulously calculated using descriptive statistics to assess the intra-fraction variation in patients, accounting for both tumor motion and setup errors. These metrics provide a clear indication of the typical positional variability that patients might experience during treatment, thereby enhancing confidence in the study's findings.

The descriptive statistics of the differences in centroid positions between the fractions of patients, obtained from 4DCBCT, are as follows:

Right-Left (RL) Direction:

- Mean difference: 0.017 cm
- Standard deviation: 0.301 cm
- Range: -0.70 cm to 0.72 cm
- Median: 0.06 cm

Superior-Inferior (SI) Direction:

- Mean difference: -0.001 cm
- Standard deviation: 0.300 cm
- Range: -0.50 cm to 0.88 cm
- Median: 0.00 cm

Anterior-Posterior (AP) Direction:

- Mean difference: -0.081 cm
- Standard deviation: 0.207 cm
- Range: -0.42 cm to 0.27 cm
- Median: -0.07 cm

The analysis reveals that the most significant tumor motion occurred in the Si direction. The mean differences in centroid positions of each fraction of 4DCBCTs are relatively small, with the largest mean difference observed in the AP direction. The standard deviations of the set-up uncertainties and tumor motion based on 4DCBCTs indicate variability in the differences, with the RL and SI directions showing higher variability than

the AP direction. The ranges of differences highlight the potential for significant deviations in individual cases, emphasizing the need for precise alignment and verification in radiotherapy to ensure accurate dose delivery.

If we take a look in more detail in this table, we can evaluate and understand some important issues:

For lesion 2, the GTV volume ranges from 0.634 cc to 0.749 cc across four fractions, with the ITV centroid positions showing substantial differences, particularly in the RL direction.

Lesion 5: This lesion shows a broader range of GTV volumes, from 10.896 cc to 14.082 cc over eight fractions. The ITV centroid positions exhibit consistent variations, especially in the RL and SI dimensions.

Lesion 18: This patient presents with one of the largest variations in GTV volume, from 16.004 cc to 35.526 cc over four fractions. The ITV centroid positions show considerable variation, particularly in the RL and SI directions.

Lesion 21: The data for lesion 12 reveals significant fluctuations in GTV volume, ranging from 2.845 cc to 3.796 cc across four fractions. The ITV centroid positions also vary widely, indicating substantial movement in the RL and SI directions.

According to the results above, patients with lesions numbered 2, 5, 18, and 21 have tumors located in the diaphragm, chest wall, and central areas. In these cases, intra-fraction deviations were found to be larger compared to other patients. We interpreted this as being due to the tumor location and the inability of the 4DCBCT to distinguish soft tissue density when performing mask matching. Therefore, while this includes errors made by the radiation oncologist when delineating the tumor on the 4DCBCT, we can also say that during the setup, the 4DCBCT has difficulty distinguishing tumors in areas close to the diaphragm and chest wall.

4.1.2. The Motion Amplitude Vector Evaluation Versus Tumor Localization

For each treatment fraction, the centroid positions of the GTV volume, as determined by 4DCBCT, were identified in the x, y, and z directions. Subsequently, the maximum coordinates in these directions—specifically the right-left (RL), superior-inferior (SI), and anterior-posterior (AP) directions—were determined. These maximum coordinate values

were then utilized to calculate the V variation value, as defined by equation (1), to quantify the deviation from the centroid position of the ITV volume determined by 4DCT.

The calculated V variation value represents the extent of deviation for each coordinate direction, providing a comprehensive measure of positional differences between the GTV in 4DCBCT and the ITV in 4DCT. This analysis aims to capture the influence of intra-fraction motion and setup errors on the positional accuracy of the target volume. Using Equation (1), the motion amplitude value V was calculated in millimeters.

Additionally, graphical representations were created to visualize the maximum centroid position coordinate values in each direction (RL, SI, and AP) as observed in the 4D CBCT scans. These graphs offer a clear depiction of the positional variability and highlight the maximum deviations encountered during the treatment process, thereby enhancing the understanding of spatial uncertainties in SBRT applications for mobile tumors. Furthermore, a comprehensive statistical analysis was conducted to evaluate the data, employing various statistical methods and techniques to ensure a thorough examination of the results and their implications.

The following figures 4.1, 4.2, and 4.3 show the V values and their respective standard deviations in the RL, SI, AP directions.

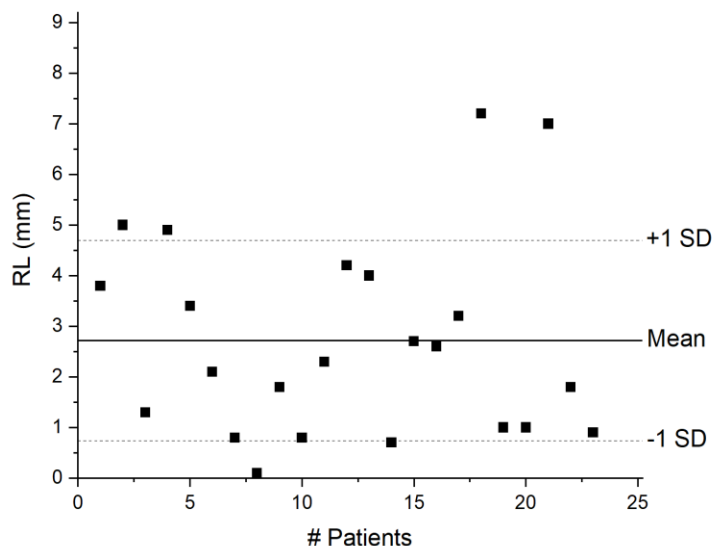


Figure 4.1. The standard deviation in the RL position

The standard deviation in the Right-Left (RL) position was calculated to have a maximum variation value of 7.2 mm and a mean value of 2.72 mm.

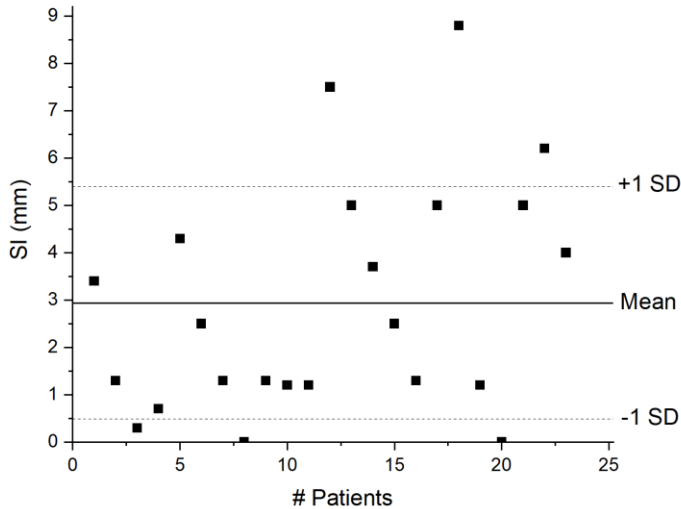


Figure 4.2. The standard deviation in the SI position

The standard deviation in the Superior-Inferior (SI) position was calculated to have a maximum variation value of 8.8 mm and a mean value of 2.94 mm.

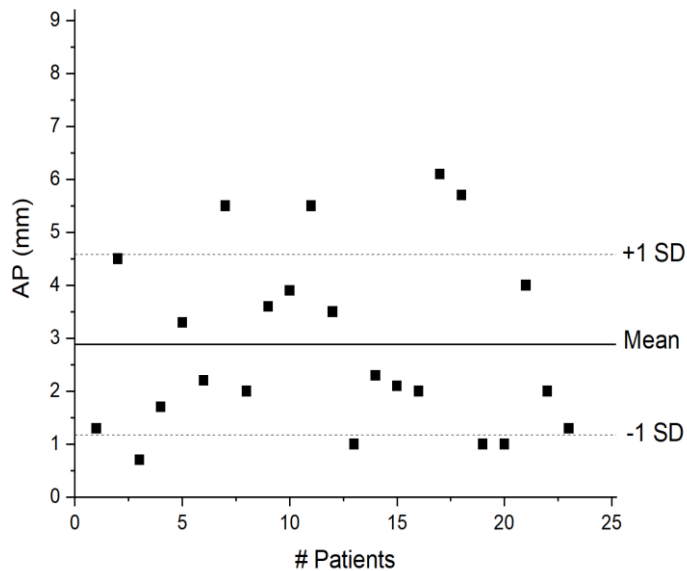


Figure 4.3. The standard deviation in the AP position

The standard deviation in the Anterior-Posterior (AP) position was calculated to have a maximum variation value of 6.1 mm and a mean value of 2.88 mm.

Table 4.2. Maximum centroid variation, mean variation values in the RL, SI, and AP coordinates, and the number of lesions greater than 5 mm.

Variation	RL (mm)	SI (mm)	AP (mm)
Mean	2.72	2.94	2.88
Maksimum centroid	7.2	8.8	6.1
Lesion number $\geq 5mm$	3	6	4

As can be seen in the table 4.2 and figures 4.1, 4.2, 4., the number of patients with variations greater than 5mm was observed to be the least in the right-left direction and the most in the superior-inferior direction.

The explanation for V_{max} is that the maximum values of V calculated using Equation (1) represent the magnitude of the motion and setup differences between the two centers. The largest V_{max} value was calculated to be 12.12 mm in the patient with lesion number 18.

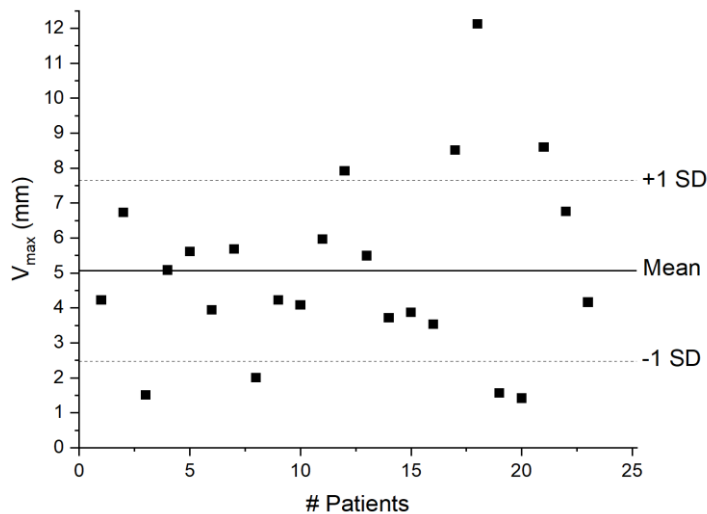


Figure 4.4. The standard deviation of V_{max}

Table 4.3 V_{max} (mm), Tumor localization and Zone classification values of lesions

Lesion	V_{max} (mm)	Tumor Localization	Zone Classification
1	4.42	LML	Central
2	6.73	LUL	Chest-wall
3	1.51	LUL	Peripheral
4	5.08	RML	Chest-wall
5	5.61	LML	Central
6	3.94	RUL	Peripheral
7	5.69	RUL	Peripheral
8	2	LUL	Peripheral
9	4.23	RUL	Peripheral
10	4.09	LLL	Peripheral
11	5.96	RML	Central
12	7.92	RLL	Peripheral
13	5.49	RUL	Peripheral
14	3.72	RUL	Central
15	3.87	RML	Peripheral
16	3.53	LLL	Peripheral
17	8.51	LUL	Peripheral
18	12.12	RLL	Diaphragm
19	1.56	LUL	Peripheral
20	1.41	LUL	Central close to heart
21	8.60	RLL	Chest-wall
22	6.76	LLL	Diaphragm
23	4.16	LUL	Chest-wall

In Table 4.3, the lesions with $V_{max} > 5$ mm values are as follows:

- Lesion number 2 is located in the Left Upper Lobe (LUL) chest wall zone.
- Lesion number 4 is located in the Right Middle Lobe (RML) chest wall zone.
- Lesion number 5 is located in the Left Middle Lobe (LML) central zone.
- Lesion number 7 is located in the Right Upper Lobe (RUL) peripheral zone.
- Lesion number 11 is located in the RML central zone.
- Lesion number 12 is located in the Right Lower Lobe (RLL) peripheral zone.

- Lesion number 13 is located in the RUL peripheral zone.
- Lesion number 17 is located in the LUL peripheral zone.
- Lesion number 18 is located in the RLL diaphragm zone.
- Lesions number 21 and 22 in the same patient are located in the RLL chest wall zone and Left Lower Lobe (LLL) diaphragm zone, respectively.

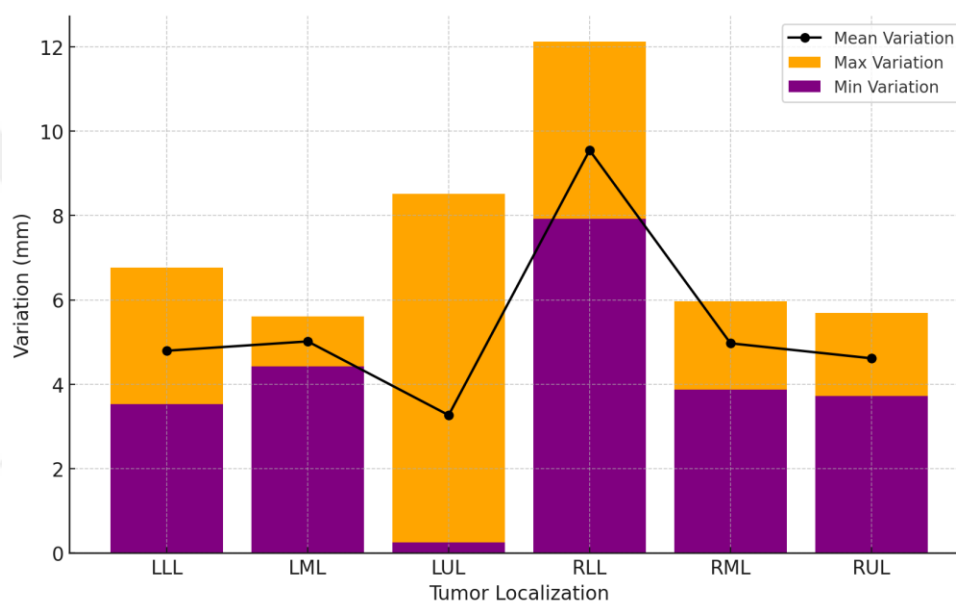


Figure 4.5. Comparison of Maximum Variations by Tumor Localization

This comparison shows the variations in GTV localization based on different tumor locations. The Right Lower Lobe (RLL) exhibits the largest variations, with a maximum variation of 12.12 mm, a minimum variation of 7.92 mm, and a mean variation of 9.55 mm. This indicates more significant challenges in accurately targeting tumors in this region. Conversely, the Left Upper Lobe (LUL) shows relatively consistent variations, with a maximum variation of 8.51 mm, a minimum variation of 1.41 mm, and a mean variation of 3.70 mm, reflecting more stable targeting.

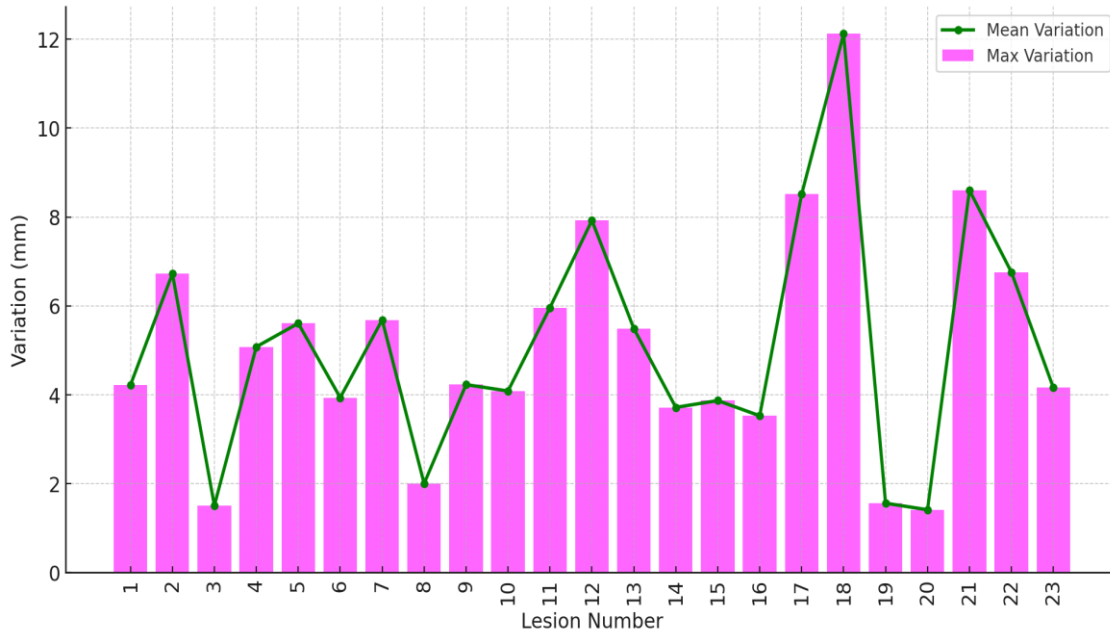


Figure 4.6. Maximum Variations in Lesion Localization of Patients

The comparison in Figure 4.5 and Figure 4.6 provides a detailed analysis of the maximum centroid variations in lesion and tumor localizations among patients. The analyses show that the maximum deviation occurred in 18 of the lesions, which are specifically located in the right lower lobe (RLL).

4.1.3. The Motion Amplitude Vector Evaluation Versus Tumor Volume

The table 4.4 presents data from this study evaluating the localization accuracy of the Planning Target Volume (PTV) in Stereotactic Body Radiotherapy (SBRT) applications using Volumetric Modulated Arc Therapy (VMAT) for mobile tumors. The study totally involves 23 lesions in 19 patients who underwent SBRT, with each patient represented by rows of data detailing variations (V_{max}) in millimeters, Internal Target Volume (ITV) in cubic centimeters (CC), fraction numbers, and Mean Gross Tumor Volume (GTV_{ADCBCT}) in cubic centimeters (CC), capturing the dynamic nature of tumor and target volumes.

Table 4.4 Comparison The Variation between ITV (cc) and mean GTV_{4DCBCT} Volume (cc)

Lesion	$V_{max}(mm)$	ITV Volume (cc)	Fraction Number	Mean $GTV_{x-4DCBCT}$ volume (cc)
1	4.42	4.958	5	3.992
2	6.73	0.524	4	0.685
3	1.51	0.715	1	0,549
4	5.08	22.512	4	11.078
5	5.61	11.081	8	12.283
6	3.94	7.335	3	4.339
7	5.69	1.357	3	0.936
8	2	0.754	1	0,541
9	4.23	1.376	1	0,754
10	4.09	0.428	3	0.415
11	5.96	9.321	5	12.597
12	7.92	11.270	5	14.406
13	5.49	32.569	5	37.702
14	3.72	29.371	3	21.676
15	3.87	6.949	3	4.896
16	3.53	3.563	3	4.634
17	8.51	3.99	3	4.312
18	12.12	55.445	4	26.105
19	1.56	0.25	3	0.268
20	1.41	0.947	3	0.492
21	8.60	3.219	4	3.253
22	6.76	4.548	3	6.276
23	4.16	1.203	3	1.826

Based on the table, we observed 12 lesions where the ITV volume was greater than the mean GTV_{4DCBCT} G volume. Additionally, we identified 7 lesions with an ITV volume V_{max} greater than 5 mm. The specific lesions where the ITV volume exceeded both the mean GTV_{4DCBCT} volume and had a V_{max} greater than 5 mm were lesions numbered 4, 7, and 18. The tumor locations for these specific lesions were as follows: Lesion number 4 was located in the chest wall, lesion number 7 was a peripheral tumor, and lesion number 18 was located near the diaphragm.

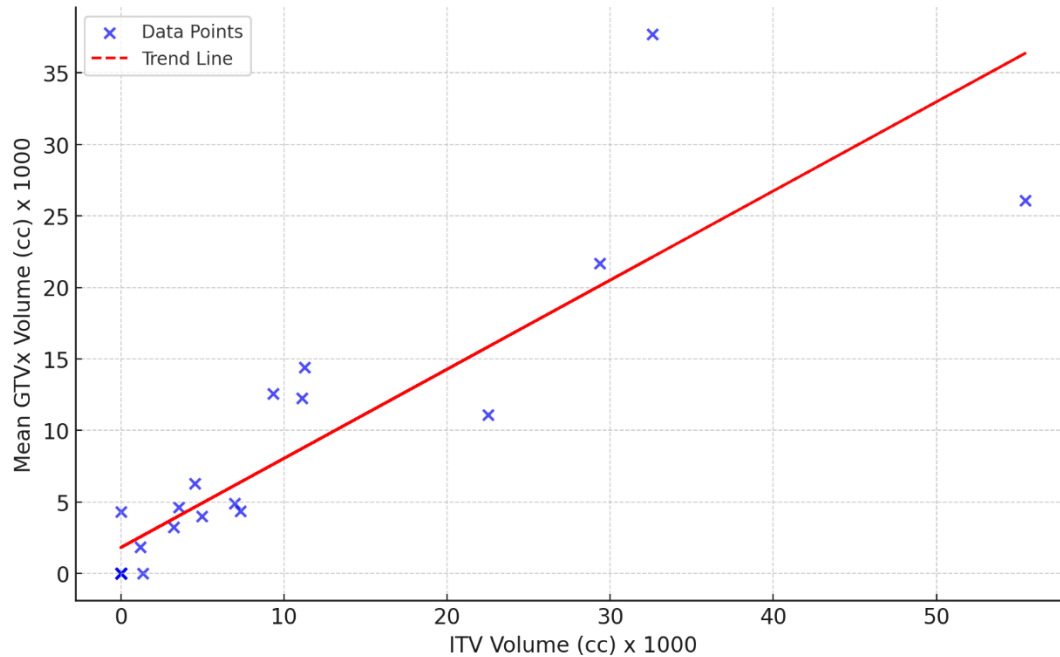


Figure 4.7. ITV Volume Vs Mean GTV_{4DCBCT} Volume with Trend Line

The graph demonstrates a generally positive correlation between ITV volume and mean GTV_{4DCBCT} volume. This implies that as the ITV volume increases, the mean GTV_{4DCBCT} volume also increases. However, there is some variability in the data points, suggesting that the relationship is not always direct. We reviewed the mean and standard deviation values of ITV volume for each region to identify the ITV volumes where deviations occurred.

Large volume ITVs (e.g., RLL and RUL):

- **RLL:** Mean 33.357 cc, Standard Deviation 31.236 cc
- **RUL:** Mean 12.308 cc, Standard Deviation 14.699 cc
- **RML:** Mean 12.927 cc, Standard Deviation 8.384 cc

Small volume ITVs (e.g., LUL):

- **LLL:** Mean 2.703 cc, Standard Deviation 2.392 cc
- **LUL:** Mean 0.172 cc, Standard Deviation 0.454 cc

As seen large and small volume ITVs, the standard deviation values are much higher for large volume ITVs (e.g., RLL and RUL), indicating that the variability is greater in large volume ITVs.

Additionally, the datasets in Table 4.4 provide a comprehensive overview of the spatial accuracy and volume consistency of tumor targeting, which is crucial for improving treatment outcomes in radiotherapy. For example, when looking at Table 4.1, patient 1 exhibited a variation (V) ranging from 2.47 mm to 4.22 mm over five fractions, with GTV volumes fluctuating between 2.657 cc and 4.757 cc. Such data help evaluate the consistency of tumor targeting and the effectiveness of the treatment plan over time.

The bar chart below displays the Mean Gross Tumor Volume (GTV) in cubic centimeters (CC) for different lesion. Each bar represents a lesion, with the height of the bar corresponding to its GTV volume. This visualization helps identify the variation in tumor volumes among the patients, highlighting any significant differences.

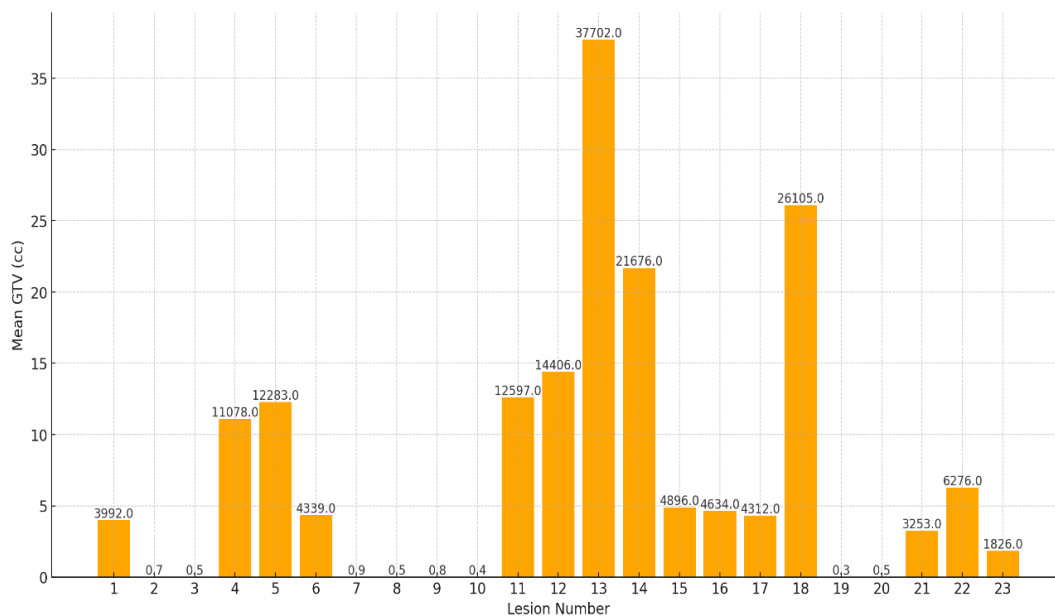


Figure 4.8. Mean GTV Volumes Across Different Lesions

4.1.4. The Evaluation of Motion Amplitude Vector in Relation to Age

Based on the analysis of the patient data, the largest variation in the dataset was observed in a 69-year-old patient, with a variation of 12.12 mm. Conversely, the smallest variation was found in an 36-year-old patient, with a variation of 1.41 mm. The data points indicate no simple linear relationship between age and variation.

Table 4.5. Comparison V_{max} and Age

Lesion	VMax (mm)	AGE	Lesion	VMax (mm)	AGE
1	4.42	73	13	5.49	55
2	6.73	82	14	3.72	77
3	1.51	68	15	3.87	56
4	5.08	64	16	3.53	66
5	5.61	36	17	8.51	75
6	3.94	68	18	12.12	69
7	5.69	82	19	1.56	36
8	2	75	20	1.41	36
9	4.23	75	21	8.60	82
10	4.09	58	22	6.76	82
11	5.96	67	23	4.16	76
12	7.92	65			

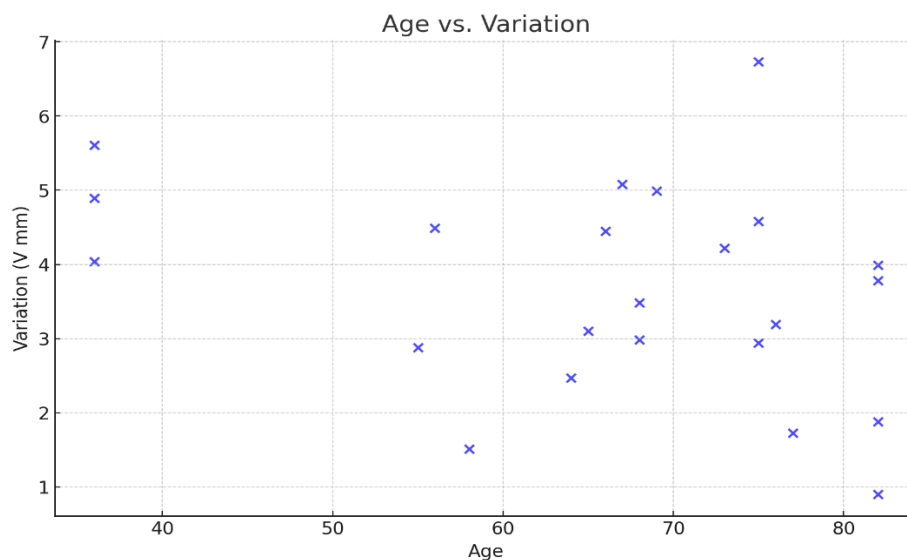


Figure 4.9. Age and V_{max} Variation

The scatter plot shows the relationship between age and variation (V) among the patients. The data points indicate no simple linear relationship between age and variation.

4.1.5. The Evaluation of Motion Amplitude Vector in Relation to Sex

The table below provides a comparison of V_{max} values between males(M) and females (F).

Table 4.6. Comparison V_{max} and Sex

Lesion	VMax (mm)	SEX	Lesion	VMax (mm)	SEX
1	4.42	M	13	5.49	M
2	6.73	M	14	3.72	M
3	1.51	M	15	3.87	M
4	5.08	F	16	3.53	M
5	5.61	F	17	8.51	M
6	3.94	M	18	12.12	M
7	5.69	M	19	1.56	F
8	2	M	20	1.41	F
9	4.23	M	21	8.60	F
10	4.09	F	22	6.76	F
11	5.96	F	23	4.16	M
12	7.92	M			

The analysis of gender-based variations in V_{max} localization revealed distinct differences between male and female patients. Female patients exhibited a maximum variation of 8.60 mm and a minimum variation of 1.41 mm, with a mean variation of 4.88 mm (standard deviation: 2.47 mm) and a median variation of 5.35 mm. In contrast, male patients showed a maximum variation of 12.12 mm and a minimum variation of 1.51 mm, with a mean variation of 5.19 mm (standard deviation: 2.72 mm) and a median variation of 4.23 mm. Males have a slightly higher mean V_{max} value compared to females, but both groups exhibit a wide range of values.

4.2. Summary Statistics and Analysis

The patients included in the study spanned ages from 36 to 82, representing a diverse age group undergoing treatment. ITV volumes ranged from 0.25 cc to 55.445 cc, while mean GTV_x volumes ranged from 0.268 cc to 37.702 cc. Additionally, PTV volumes reflected margins between 3mm and 7mm added to the ITV for treatment planning.

Statistical significance was assessed using SPSS version 25.0. We utilized a paired t-test and the Pearson correlation formula to examine relationships, setting the threshold for significance at $p > 0.05$.

- **ITV Volume and Vmax:** We explored the relationship between ITV volume and Vmax and found it to be significant ($p:0.01$). A large ITV volume was linked to a large standard deviation, suggesting that the determination of the PTV margin could be based on the size of the ITV. However, ITV volume alone is not the sole criterion for determining the PTV margin; tumor location is also a critical factor.
- **Tumor's Direction:** The tumor location was found to be largest in the SI direction. Despite observing the maximum deviation in the SI direction, tumor location and Vmax were not statistically significant. ($p=0.59$)
- **Vmax and Zone Classification:** No significant relationship was found between Vmax and zone classification, specifically proximity to the diaphragm - chest wall.
- **Vmax and Tumor Localization (e.g., RLL):** No significant relationship was found between Vmax and tumor localization, such as RLL.
- **Vmax and Age:** No significant relationship was found between Vmax and age.
- **Vmax and Sex:** No significant relationship was found between Vmax and sex.

Progress in radiotherapy has led to the development of Intensity-Modulated Radiation Therapy (IMRT) and Volumetric Modulated Arc Therapy (VMAT) for Linac-based Stereotactic Body Radiation Therapy (SBRT). These advancements allow us to precisely shape the distribution of radiation dose around the tumor, while minimizing the exposure of critical organs. The high dose conformity, which is essential for the delivery of high ablative radiation doses to lung tumors in a few fractions by SBRT, requires improved targeting accuracy. However, this accuracy is impeded by organ motions at multiple locations of the tumor, which are classified as intrafractional and interfractional motions. These motions, particularly for lung tumors, result in geometric and dosimetric uncertainties in the radiotherapy treatment, as patient-specific respiratory movement causes variance in tumor position^(10,15). Hence, in the case of lung SBRT, precise management of respiratory motion is crucial to ensure the accurate administration of the prescribed dose to the tumor. The published data has demonstrated that the accuracy of tumor targeting may be compromised by the potential underestimation of the range of tumor motion by free-breathing 3DCBCT imaging^(6,10). By considering bone structure, CBCT imaging effectively addresses inter- and intra-fractional tumor variation and setup variation. However, factors such as tumor size and patient characteristics also play a significant role in determining patients' set-up margins, although they have a minimal impact on the set-up margin itself. These factors don't have much of an effect on the set-up margin, but new data shows (abulimiti et al)⁽⁴⁹⁾ that using the right protocols for the 4dcbct in lung SBRT can fix the problem of motion and accurately define the target position. The 4DCBCT dataset uses on-board treatment verification imaging to determine the patient's individual breathing pattern, which is crucial for acquiring lesion motion data. This method provides a significant advantage in reducing uncertainties in motion, allowing for accurate determination of tumor position prior to or during each treatment session.

The precise estimation of tumor volume by respiratory-correlated fan beam CT (4DCT) and respiratory-correlated cone beam CT (4DCBCT) is essential for the accurate dosimetry and treatment verification of lung stereotactic body radiation therapy (SBRT) and other motion-managed therapies. Both 4DCT and 4DCBCT are frequently employed in

external beam radiation therapy. Patients employ 4DCT for patient simulation and treatment planning, and 4DCBCT for patient treatment. The gold standard for positional correction in imaging-guided radiotherapy (IGRT) is 4DCBCT, which incorporates respiratory motion data. This method allows for the real-time monitoring of target area motion and patient setup errors. The standard for delineating the intended treatment volume (ITV) throughout the respiratory cycle in precision radiotherapy for lung cancer has been established by 4DCT⁽⁶⁾. Nevertheless, it is widely recognized that the two modalities may exhibit discrepancies due to the fact that 4DCT and 4DCBCT differ in certain aspects of image acquisition and reconstruction. The quantitative assessment of the distinctions between 4DCT and 4DCBCT imaging during respiratory motion could be beneficial for enhancing the definition of internal target and planning target volume margins. Thus, we examined the precision and disparities in volume for tumors located in different regions of the lung, such as the lower and upper lobes, and those attached to the chest wall or diaphragm. This was done by comparing the volume outlined by ITV on 4DCT scans and the volume measured by GTV_x on 4DCBCT imaging. We also examined the relationship between tumor volume and the variation in the centroid position of the tumor.

According to the data presented in Table 4.4, we identified 12 instances where the volume of the internal target volume (ITV) was larger than the average volume of the gross tumor volume (GTV_x). In addition, we have detected 7 lesions with an ITV volume V_{max} exceeding 5 mm. This finding is statistically associated with variations in tumor volume and the amplitude of centroid position, which aligns with the research conducted by Abullimiti et al. The particular abnormalities that surpassed both the average volume of the gross tumor volume (GTV_x) and had a maximum volume (V_{max}) greater than 5 mm were lesions situated in the chest wall and in close proximity to the diaphragm. Lee et al.⁽⁵⁵⁾ demonstrate that the 4DCBCT dataset of the lung tumor can more precisely determine the tumor volume compared to the 4DCT images, as evidenced by the phantom study. In a recent thesis, we found similar outcomes to those reported by Lee et al., showing that we can determine the size of a tumor by analyzing patient 4dCBCT images for SBRT lung treatment. This analysis considers the individual patient's breathing pattern and the location of the tumor.

The respiration motion analysis was performed by comparing and calculating the centroid position of each fraction's respective GTV_x, which was obtained from 4DCBCT

data in patients who were treated with stereotactic radiotherapy for lung cancer. In the recent thesis, we indicated the tumor position variation as the centroid position variation (V_{xyz}) for each direction and V_{max} as a vector of the magnitude of variation of the corresponding GTVx. The statistical description of the variations in centroid positions between the fractions of patients obtained from 4DCBCT indicate that our findings align with the published data by Takahashi et al. ⁽⁵⁹⁾, which states that the variation in centroid tumor position was below 10 mm in all directions. The mean displacements between the initial target volume (ITV) and the actual tumor location, as measured by the 4-dimensional cone-beam computed tomography (4DCBCT) scans obtained prior to each treatment, were 0.017 ± 0.301 cm in the right-left (RL) direction, 0.001 ± 0.3 cm in the superior-inferior (SI) direction, and 0.081 ± 0.207 cm in the anterior-posterior (AP) direction, respectively. The standard deviations of the intra fraction movements, encompassing the uncertainties in set-up based on 4DCBCT, along with the motion of the tumor, demonstrate variability in the disparities. The distribution of translation displacements for each patient were reported in Figure 4.1, 4.2, and 4.3. The RL and SI directions exhibit greater variability compared to the AP direction. The standard deviation in the Superior-Inferior (SI) position was calculated to have a maximum variation value of 8.8 mm and a mean value of 2.94 mm. While our sample size was insufficient for making broad conclusions, our examination of 23 lesions in various areas of the lung yielded findings that aligned with existing literature. According to table 4.2 and figures 4.1, 4.2, and 4.3, the fewest number of patients with variations greater than 5mm was observed in the right-left direction, while the highest number was observed in the superior-inferior direction. The analysis depicted in Figures 4.5 and 4.6 provides a thorough comparison of the greatest deviations in the positions of lesions and tumors' centroids across patients. The analyses indicate that the most significant deviation was observed in the lesions, which are specifically located in the right lower lobe (RLL).

Furthermore, our evaluation of V_{max} deviation in relation to tumor localization reveals that intra-fraction deviations are more significant in patients with larger tumor volumes located in the lower lobe, particularly when the tumor is adhered to the chest wall and diaphragm.

The potential weaknesses of the recent thesis are the small sample size of patients and GTVx, which were obtained from the delineation of 4DCBCT by the same radiation

oncologist. This could lead to errors caused by registration inaccuracies and a lack of independent observation by another physician. Furthermore, it is crucial to consider the potential error that can occur due to the tumor's position and the limited ability of 4DCBCT to differentiate soft tissue density during mask alignment. Thus, in addition to the mistakes made by the radiation oncologist in outlining the tumor on the 4DCBCT, it can be stated that the 4DCBCT encountered challenges in identifying tumors located near the diaphragm and chest wall during the setup process.

The results of our study align with those of Li et al. ⁽⁶⁰⁾, who showed that a standard 1 cm margin in the SI plane is inadequate to accommodate the varied shapes of tumors when using 3DCBCT for tumor localization. However, our findings confirm that a 1 cm margin is adequate in our cases. Additionally, a 0.5 cm margin is sufficient in the RL and AP directions, but not in the SI direction, to encompass the motion of the tumor, which is located in the lower lobe and attached to the chest wall and diaphragm. The significance of precise alignment, assessment of patients' unique breathing patterns, and validation in radiotherapy is underscored by the variations in differences, which underscore the possibility of substantial deviations in individual cases. This is necessary to ensure the precise administration of the prescribed dose and to establish a sufficient margin for each direction of the tumor.

Based on our initial observations, the acquisition of 4DCBCT with Symmetry Elekta X-Ray software appears to be a valuable approach for assessing organ motion in thoracic stereotactic radiotherapy. In order to verify these data and to examine the optics of personalizing the PTV margin, it is undoubtedly necessary to increase the number of patients.

REFERENCES

1. Arimura H. *Image-Based Computer-Assisted Radiation Therapy*. Springer Singapore; 2017. doi:10.1007/978-981-10-2945-5
2. Bernier J, Hall EJ, Giaccia A. Radiation oncology: A century of achievements. *Nat Rev Cancer*. 2004;4(9):737-747. doi:10.1038/nrc1451
3. Park K. The mixed era of stereotactic radiosurgery and radiotherapy. *J Korean Soc Stereotact Funct Neurosurg*. 2021;17(1):6-13. doi:10.52662/jksfn.2021.00038
4. Zwiggelaar R, Bull CR, Mooney MJ, Sonia ;, Oe C. *The Detection of “Soft” Materials by Selective Energy Xray Transmission Imaging and Computer Tomography*. Vol 66.; 1997.
5. Chan C, Lang S, Rowbottom C, Guckenberger M, Faivre-Finn C. Intensity-modulated radiotherapy for lung cancer: Current status and future developments. *J Thorac Oncol*. 2014;9(11):1598-1608. doi:10.1097/JTO.0000000000000346
6. Slotman BJ, Lagerwaard FJ, Senan S. 4D imaging for target definition in stereotactic radiotherapy for lung cancer. In: *Acta Oncologica*. Vol 45. ; 2006:966-972. doi:10.1080/02841860600902817
7. Zhao N, Yang R, Wang J, Zhang X, Li J. An IMRT/VMAT Technique for Nonsmall Cell Lung Cancer. *Biomed Res Int*. 2015;2015. doi:10.1155/2015/613060
8. Rusthoven KE, Pugh TJ. Stereotactic body radiation therapy for inoperable lung cancer. *Jama*. 2010;303(23):2354-2355. doi:10.1001/jama.2010.777
9. Aznar MC, Warren S, Hoogeman M, Josipovic M. The impact of technology on the changing practice of lung SBRT. *Phys Medica*. 2018;47:129-138. doi:10.1016/j.ejmp.2017.12.020
10. Brandner ED, Chetty IJ, Giaddui TG, Xiao Y, Huq MS. Motion management strategies and technical issues associated with stereotactic body radiotherapy of thoracic and upper abdominal tumors: A review from NRG oncology. *Med Phys*. 2017;44(6):2595-2612. doi:10.1002/mp.12227
11. Brown AM, Mak RH, Kann BH. Advances in stereotactic body radiation therapy for early stage non-small cell lung cancer. 2022;(3):1-12. doi:10.21037/ccts-21-16
12. Benedict SH, Yenice KM, Followill D, et al. Stereotactic body radiation therapy: The report of AAPM Task Group 101. *Med Phys*. 2010;37(8):4078-4101. doi:10.1118/1.3438081
13. TASAKI Y, ASHIZAWA K, NAKAMURA D, et al. Clinical Outcomes of Stereotactic Body Radiation Therapy for Early-stage Non-small Cell Lung Cancer. *Cancer Diagnosis Progn*. 2023;3(2):201-207. doi:10.21873/cdp.10202
14. Wu J, Betzing C, He TT, Fuss M, D'Souza WD. Dosimetric comparison of patient setup strategies in stereotactic body radiation therapy for lung cancer. *Med Phys*. 2013;40(5). doi:10.1118/1.4801926
15. Reddy BNS, Shivananjappa R, S.N G, Tiwari R. Use of 4-Dimensional Cone Beam Computed Tomography Scan to Estimate the Planning Target Volume Margin in Lung Tumors. *Asian J Oncol*. 2020;06:127-133. doi:10.1055/s-0040-1714304
16. Wang L, Feigenberg S, Fan J, et al. Target repositional accuracy and PTV margin verification using three-dimensional cone-beam computed tomography (CBCT) in stereotactic body radiotherapy (SBRT) of lung cancers. *J Appl Clin Med Phys*. 2012;13(2):41-54. doi:10.1120/jacmp.v13i2.3708

17. Li Y, Ma J lu, Chen X, Tang F wen, Zhang X zhi. 4DCT and CBCT based PTV margin in Stereotactic Body Radiotherapy(SBRT) of non-small cell lung tumor adhered to chest wall or diaphragm. *Radiat Oncol.* 2016;11(1). doi:10.1186/s13014-016-0724-5
18. Zhang Y, Feng Y, Wang W, Yang C, Wang P. An Expanded Multi-scale Monte Carlo Simulation Method for Personalized Radiobiological Effect Estimation in Radiotherapy: A feasibility study. *Sci Rep.* 2017;7. doi:10.1038/srep45019
19. Molitoris JK, Diwanji T, Snider JW, et al. Advances in the use of motion management and image guidance in radiation therapy treatment for lung cancer. *J Thorac Dis.* 2018;10:S2437-S2450. doi:10.21037/jtd.2018.01.155
20. Keall PJ, Mageras GS, Balter JM, et al. The management of respiratory motion in radiation oncology report of AAPM Task Group 76. *Med Phys.* 2006;33(10):3874-3900. doi:10.1118/1.2349696
21. Simon S. Lo, Bin S. Teh, Jiade J. Lu TES. *Stereotactic Body Radiation Therapy.* (Luther W. Brady, Hans-Peter Heilmann, Michael Molls CN, ed.). Springer-Verlag Berlin Heidelberg; 2012. doi:10.1007/978-3-642-25605-9
22. Amini A, Yeh N, Gaspar LE, Kavanagh B, Karam SD. Stereotactic body radiation therapy (SBRT) for lung cancer patients previously treated with conventional radiotherapy: A review. *Radiat Oncol.* 2014;9(1). doi:10.1186/1748-717X-9-210
23. Iovoli AJ, Yu B, Ma SJ, et al. Quality of Life After Stereotactic Body Radiation Therapy or Surgery for Early-Stage NSCLC: A Systematic Review. *JTO Clin Res Reports.* 2022;3(11):100417. doi:10.1016/j.jtocrr.2022.100417
24. Bezjak A, Paulus R, Gaspar LE, et al. *Safety and Efficacy of a Five-Fraction Stereotactic Body Radiotherapy Schedule for Centrally Located Non-Small-Cell Lung Cancer: NRG Oncology/RTOG 0813 Trial.* Vol 37.; 2019. <https://doi.org/10.1016/j.jtocrr.2022.100417>
25. Videtic GMM, Hu C, Singh AK, et al. A randomized phase 2 study comparing 2 stereotactic body radiation therapy schedules for medically inoperable patients with stage I peripheral non-small cell lung cancer: NRG Oncology RTOG 0915 (NCCTG N0927). In: *International Journal of Radiation Oncology Biology Physics.* Vol 93. Elsevier Inc.; 2015:757-764. doi:10.1016/j.ijrobp.2015.07.2260
26. Chi A, Nguyen NP, Komaki R. The potential role of respiratory motion management and image guidance in the reduction of severe toxicities following stereotactic ablative radiation therapy for patients with centrally located early stage non-small cell lung cancer or lung metastases. *Front Oncol.* 2014;4 JUN(June):1-12. doi:10.3389/fonc.2014.00151
27. Chinneck CD, McJury M, Hounsell AR. The potential for undertaking slow CT using a modern CT scanner. *Br J Radiol.* 2010;83(992):687-693. doi:10.1259/bjr/31551018
28. Abdelnour AF, Nehmeh SA, Pan T, et al. Phase and amplitude binning for 4D-CT imaging. *Phys Med Biol.* 2007;52(12):3515-3529. doi:10.1088/0031-9155/52/12/012
29. Pan T. Comparison of helical and cine acquisitions for 4D-CT imaging with multislice CT. *Med Phys.* 2005;32(2):627-634. doi:10.1118/1.1855013
30. Zhang F, Kelsey CR, Yoo D, Yin FF, Cai J. Uncertainties of 4-dimensional computed tomography-based tumor motion measurement for lung stereotactic body radiation therapy. *Pract Radiat Oncol.* 2014;4(1):e59-e65. doi:10.1016/j.prro.2013.02.009
31. Davey A, Van Herk M, Faivre-Finn C, Brown S, McWilliam A. Optimising use of 4D-CT phase information for radiomics analysis in lung cancer patients treated with stereotactic body radiotherapy. *Phys Med Biol.* 2021;66(11). doi:10.1088/1361-6560/abfa34
32. Wang G, Zhu X, Zhang F, et al. Applied research of a four-dimensional CT localization technique in radiotherapy and treatment planning for early lung cancer. *Transl Cancer Res.*

- 2020;9(11):7227-7235. doi:10.21037/tcr-20-2800
33. Sweeney RA, Seubert B, Stark S, et al. Accuracy and inter-observer variability of 3D versus 4D cone-beam CT based image-guidance in SBRT for lung tumors. *Radiat Oncol.* 2012;7(1). doi:10.1186/1748-717X-7-81
 34. Glide-Hurst CK, Chetty IJ. Improving radiotherapy planning, delivery accuracy, and normal tissue sparing using cutting edge technologies. *J Thorac Dis.* 2014;6(4):303-318. doi:10.3978/j.issn.2072-1439.2013.11.10
 35. Borm KJ, Oechsner M, Wiegandt M, Hofmeister A, Combs SE, Duma MN. Moving targets in 4D-CTs versus MIP and AIP: Comparison of patients data to phantom data. *BMC Cancer.* 2018;18(1). doi:10.1186/s12885-018-4647-4
 36. Mercieca S, Belderbos JSA, van Herk M. Challenges in the target volume definition of lung cancer radiotherapy. *Transl Lung Cancer Res.* 2021;10(4):1983-1998. doi:10.21037/tlcr-20-627
 37. Trémolières P, Gonzalez-Moya A, Paumier A, et al. Lung stereotactic body radiation therapy: personalized PTV margins according to tumor location and number of four-dimensional CT scans. *Radiat Oncol.* 2022;17(1):1-9. doi:10.1186/s13014-021-01973-5
 38. Giraud P, Houle A. Respiratory Gating for Radiotherapy: Main Technical Aspects and Clinical Benefits. *ISRN Pulmonol.* 2013;2013(Table 1):1-13. doi:10.1155/2013/519602
 39. Brock J, McNair HA, Panakis N, Symonds-Tayler R, Evans PM, Brada M. The use of the active breathing coordinator throughout radical non-small-cell lung cancer (NSCLC) radiotherapy. *Int J Radiat Oncol Biol Phys.* 2011;81(2):369-375. doi:10.1016/j.ijrobp.2010.05.038
 40. Caillet V, Booth JT, Keall P. IGRT and motion management during lung SBRT delivery. *Phys Medica.* 2017;44:113-122. doi:10.1016/j.ejmp.2017.06.006
 41. Murphy MJ, Balter J, Balter S, et al. The management of imaging dose during image-guided radiotherapy: Report of the AAPM Task Group 75. *Med Phys.* 2007;34(10):4041-4063. doi:10.1118/1.2775667
 42. Srivivasan K, Mohammadi M, Shepherd J. Applications of linac-mounted kilovoltage Cone-beam Computed Tomography in modern radiation therapy: A review. *Polish J Radiol.* 2014;79:181-193. doi:10.12659/PJR.890745
 43. Li J, Harrison A, Yu Y, Xiao Y, Werner-Wasik M. Evaluation of Elekta 4D cone beam CT-based automatic image registration for radiation treatment of lung cancer. *Br J Radiol.* 2015;88(1053). doi:10.1259/bjr.20140620
 44. Zhuang L, Yan D, Liang J, et al. Evaluation of image guided motion management methods in lung cancer radiotherapy. *Med Phys.* 2014;41(3). doi:10.1118/1.4866220
 45. Sonke JJ, Zijp L, Remeijer P, Van Herk M. Respiratory correlated cone beam CT. *Med Phys.* 2005;32(4):1176-1186. doi:10.1118/1.1869074
 46. A A, Kida S, Saotome N, et al. *Others: Four-Dimensional Cone-Beam CT during SBRT.*; 2015. doi:10.1007/978-4-431-54883-6_18
 47. Thengumpallil S, Smith K, Monnin P, Bourhis J, Bochud F, Moeckli R. Difference in performance between 3D and 4D CBCT for lung imaging: a dose and image quality. *J Appl Clin Med Phys.* 2016;17(6):97-106. doi:10.1120/jacmp.v17i6.6459
 48. Tan Z, Liu C, Zhou Y, Shen W. Preliminary comparison of the registration effect of 4D-CBCT and 3D-CBCT in image-guided radiotherapy of Stage IA non-small-cell lung cancer. *J Radiat Res.* 2017;58(6):854-861. doi:10.1093/jrr/rrx040
 49. Abulimiti M, Yang X, Li M, Huan F, Zhang Y, Jun L. Application of four-dimensional cone beam computed tomography in lung cancer radiotherapy. *Radiat Oncol.*

- 2023;18(1):1-8. doi:10.1186/s13014-023-02259-8
50. Zhang Y, Huang X, Wang J. Advanced 4-dimensional cone-beam computed tomography reconstruction by combining motion estimation, motion-compensated reconstruction, biomechanical modeling and deep learning. *Vis Comput Ind Biomed Art*. 2019;2(1). doi:10.1186/s42492-019-0033-6
 51. Iramina H, Nakamura M, Iizuka Y, et al. The accuracy of extracted target motion trajectories in four-dimensional cone-beam computed tomography for lung cancer patients. *Radiother Oncol*. 2016;121(1):46-51. doi:10.1016/j.radonc.2016.07.022
 52. Bellec J, Arab-Ceschia F, Castelli J, Lafond C, Chajon E. ITV versus mid-ventilation for treatment planning in lung SBRT: A comparison of target coverage and PTV adequacy by using in-treatment 4D cone beam CT. *Radiat Oncol*. 2020;15(1). doi:10.1186/s13014-020-01496-5
 53. Nakano M, Haga A, Kotoku J, et al. Cone-beam CT reconstruction for non-periodic organ motion using time-ordered chain graph model. *Radiat Oncol*. 2017;12(1). doi:10.1186/s13014-017-0879-8
 54. Bryce-Atkinson A, Marchant T, Rodgers J, et al. Quantitative evaluation of 4D Cone beam CT scans with reduced scan time in lung cancer patients. *Radiother Oncol*. 2019;136:64-70. doi:10.1016/j.radonc.2019.03.027
 55. Lee TC, Bowen SR, James S St., Sandison GA, Kinahan PE, Nyflot MJ. Accuracy Comparison of 4D Computed Tomography (4DCT) and 4D Cone Beam Computed Tomography (4DCBCT). *Int J Med Physics, Clin Eng Radiat Oncol*. 2017;06(03):323-335. doi:10.4236/ijmpcero.2017.63029
 56. Palma D, Vollans E, James K, et al. Volumetric Modulated Arc Therapy for Delivery of Prostate Radiotherapy: Comparison With Intensity-Modulated Radiotherapy and Three-Dimensional Conformal Radiotherapy. *Int J Radiat Oncol Biol Phys*. 2008;72(4):996-1001. doi:10.1016/j.ijrobp.2008.02.047
 57. Bedford JL, Nordmark Hansen V, Mcnair HA, et al. Treatment of lung cancer using volumetric modulated arc therapy and image guidance: A case study. *Acta Oncol (Madr)*. 2008;47(7):1438-1443. doi:10.1080/02841860802282778
 58. Han Z, Ng SK, Bhagwat MS, Lyatskaya Y, Zygmanski P. Evaluation of MatriXX for IMRT and VMAT dose verifications in peripheral dose regions. *Med Phys*. 2010;37(7):3704-3714. doi:10.1118/1.3455707
 59. Takahashi W, Yamashita H, Kida S, et al. Verification of planning target volume settings in volumetric modulated arc therapy for stereotactic body radiation therapy by using in-treatment 4-dimensional cone beam computed tomography. *Int J Radiat Oncol Biol Phys*. 2013;86(3):426-431. doi:10.1016/j.ijrobp.2013.02.019
 60. Li Y, Wu W, He R, et al. Using 4DCBCT simulation and guidance to evaluate inter-fractional tumor variance during SABR for lung tumor within the lower lobe. *Sci Rep*. 2021;11(1):1-9. doi:10.1038/s41598-021-99489-1

Curriculum Vitae

Personal Information

Name	JÜLİDE	Surname	CANBULDU

Education

Degree	Department	The name of the Institution Graduated From	Graduation year
Master	Health Physics	Yeditepe University	2024
University	Physics	Uludağ University	2005
High school	Science and Mathematics	Sakarya Anadolu High School	2000

All the grades must be listed if there is more than one (KPDS, ÜDS, TOEFL; EELTS vs),

Languages	Grades (#)
English	Intermediate

Work Experience (Sort from present to past)

Position	Institute	Duration (Year - Year)
Founder Representative	Özel Erenköy Murat İmeryüz Özel Öğretim Kursu	2014- Present